CONVERGENCE PROPERTIES of FRACTIONALLY-SPACED EQUALIZERS for DATA TRANSMISSION

by

© *M. Melih Pekiner, B.Sc.*
Bogazici University, Istanbul
Department of Electrical Engineering

A thesis submitted to the
Faculty of Graduate Studies and Research
in partial fulfillment of the requirements
for the degree of
Master of Engineering

Department of Electrical Engineering
McGill University
Montreal, Canada

ABSTRACT

This thesis considers the convergence properties of adaptive equalizers used for data transmission. In the conventional form of a tapped delay line equalizer, the tap spacing is equal to the symbol interval T. Two other cases are discussed. The fractional-spaced equalizer has tap spacing less than T ($T/2$ is considered in detail). A hybrid configuration uses both T spaced and fractional T spaced tap is also considered. From the mathematical derivations and the computer simulations the properties, the relative advantages and drawbacks of the three cases are analysed.

RESUMÉ

Cette thèse traite des propriétés de convergence des égaliseurs conventionnels dans le domaine des transmissions de données. Dans un égaliseur conventionnel la distance entre perforations correspond à l'intervalle entre symboles T. Deux autres configurations sont ici considérés: l'égaliseur à espace fractionnel dont la distance entre perforations est inférieure à T, et l'égaliseur hybride, utilisant des distances de perforation égales à T et inferieures à T. Les différentes propriétés, avantages et inconvénients des trois types d'égaliseurs sont comparés sur une base mathématique et de simulation par ordinateur.

ACKNOWLEDGEMENTS

I wish to extend my sincere thanks to Dr. P. Kabal for his guidance, and constant support in every aspect of this work; to Dr. M. Ferguson for his help in the documentation, to K. Gupta for his help in going over the text; to Dr. Y. Youssef and A. Dill for their help in creating some of the figures in this thesis; to Miss J. Chardon for her translation of the abstract; and to the Marauders for the very friendly atmosphere they have created in the office and in the computer labaratory.

And to my parents for their encouragement, financial support and continuing interest in my academic progress.

To my Parents

TABLE of CONTENTS

LIST of FIGURES

CHAPTER I

INTRODUCTION

I.1 Adaptive Equalization

Digital data transmission systems are often bandwidth limited. Moreover, the channel characteristics may change for each transaction or even during transactions. The recent applications of computer communication on the voice-bandwidth channels, and satellite channels has raised a new interest in the optimization of data transmission systems.

The transmission channel tends to degrade the transmitted signal, causing difficulties in recovering the original data. One of the sources of degradation is the additive noise due to background thermal noise or impulsive noise. This noise can be reduced to some extent by using bandpass filters to exclude out-of-band noise. Another form of degradation is the time dispersion, which extends the duration of the input signal, causing the adjacent data symbols to interfere with each other. This effect of overlapping of received symbols is called Intersymbol Interference (ISI) [R.W. Lucky, J. Salz and E.J. Weldon, 1968].

Bandwidth efficient data transmission over the real analog channels requires equalization to reduce intersymbol interference. The idea behind equalization is to reduce the cross effects between the individual symbols using the past and the future samples. In practice, the equalizer is implemented in the form of a transversal filter or a tapped delay line. The weighted outputs of the delay taps are summed to form the output of the filter. An automatic or adaptive equalizer varies these tap weights by using one of the methods described in [Gersho, 1969], [Hirsch, 1970], [Lucky, 1965, 1967], [Chang, 1971].

There are two basic kinds of adjusment procedures. The first one, often called automatic equalization, is done by sending a string of isolated test pulses before the actual data is transmitted. The equalizer tap coefficients are kept constant after this 'training' period. In the other method, 'adaptive equalization', the equalizer settings are updated directly from the received data. Adaptive equalizers minimize the degradation of the signal using, first the *a priori* known training sequence, and then an estimate of the data during transmission. When actual data transmission starts, the distortion is already reduced to a small value. At this moment, the equalizer can use the reconstructed output signal of the receiver as a reference signal. This kind of operation is usually referred to as decision-directed mode. The effect of wrong decisions is usually negligible after a successful training period.

Early equalizers used a tap spacing of T, the symbol spacing period. Recent studies on equalizers showed that further improvement in performance can be obtained using a tap time spacing of less than T. These equalizers that have tap spacing less than T are called Fractional-Tap-Spaced-Equalizers. This type of equalizer has been analysed by [Ungerboeck, 1976], [Gitlin and Weinstein, 1981], [Qureshi and Forney, 1977].

In digital data communication systems, not only are different channels used

each time a transmission is requested, but the channel itself may have time varying characteristics. A data transmission is made up of a training period which is followed by the transmission of the actual data. The start-up time is defined as the time during which the receiver locks on to the carrier, establishes bit synchronization and performs automatic equalization. This overhead takes a considerable portion of the total busy period. For the early automatic equalizers, settling times in the order of seconds have been reported. Since then great improvements have been achieved.

I.2 Thesis Overview

In this work, we study the adaptation behaviour of conventional, fractional-spaced, and hybrid equalizers. The idea of a hybrid equalizer was first proposed by P. Kabal and studied by [Nattiv, 1980].

The second chapter describes a baseband digital data communication system using passband equivalent model for the system to be studied. The problem of intersymbol interference is also discussed. The following chapter consists of an overview of optimal minimum mean-square error equalization. Chapter 3 also includes a study of an equalizer analysis with general tap spacing. In Chapter 4, the properties of the conventional, fractional-tap spaced, and hybrid equalizers are discussed in terms of their frequency characteristics, eigenvalues and minimum mean-square error. Chapter 5 starts by introducting algorithms used for the adaptive equalizers. This is followed by a summary of the steepest descent algorithm for tap adjustments. The chapter concludes with the discussion on the convergence properties of the equalizers. The description of the simulation and the results are presented in Chapter 6.

CHAPTER II

BASEBAND DATA COMMUNICATION SYSTEM

II.1 Model of Digital Communication System

The structure of a digital communication system can be modelled as in Figure 2.1. The three main blocks are the transmitter, the channel and the receiver. The source symbols at every T second intervals are passed through a bandlimited filter whose impulse response is $h_s(t)$, and $g_T(t)$ is generated at the output of the transmitter,

$$g_T(t) = \sum_n a_n h_s(t - nT). \tag{2.1}$$

This signal is fed to the channel which is viewed as a filter of impulse response $h_m(t)$. Random noise $n_r(t)$ is added by the channel and the final form of the signal is,

$$g_R(t) = g_T(t) * h_m(t) + n_r(t). \tag{2.2}$$

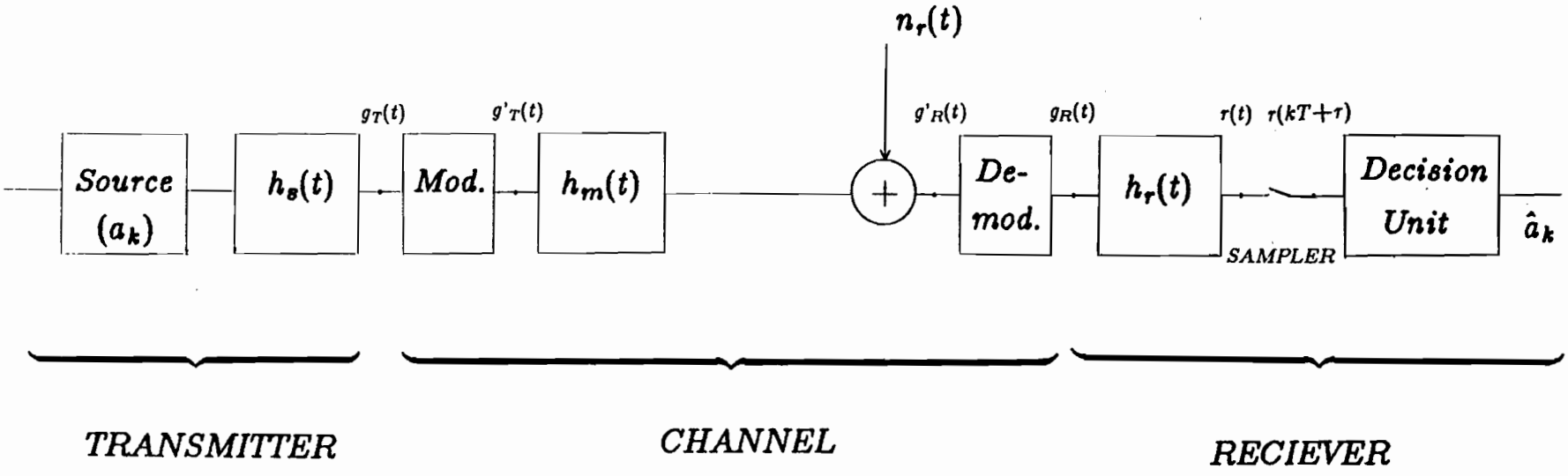

Figure 2.1 Structure of a Communication System.

This received signal passes through the receiver block which consists of three parts a filter, a sampler and a decision unit. The same model serves to study modulated passband systems. In this case the parameters take on complex values, representing the quadrature and in phase components of the baseband equivalent parameters.

Before the sampler, the signal is of the form,

$$r(t) = \sum_n a_n h(t - nT) + n(t), \tag{2.3}$$

where

$$h(t) = h_s(t) * h_m(t) * h_r(t), \tag{2.4}$$

and

$$n(t) = n_r(t) * h_r(t). \tag{2.5}$$

The sampled signal is given by,

$$r(kT) = \sum_n a_n h(kT - nT + \tau) + n(kT + \tau). \tag{2.6}$$

The sampler is assumed to be in synchrony with the symbol interval but with a time offset τ . Define

$$r_k \triangleq r(kT + \tau), \tag{2.7a}$$

$$h_{k-n} \triangleq h(kT - nT + \tau), \tag{2.7b}$$

$$n_k \triangleq n(kT + \tau). \tag{2.7c}$$

Then

$$r_k = \sum_n a_n h_{n-k} + n_k, \tag{2.8}$$

are the samples input at the decision unit. The sampling time is offset by τ with respect to source clock. The final block outputs a symbol $\hat{a_k}$ which is an estimate of the input at the source.

When one starts to look at optimizing the above system, the approach might be either to optimize the transmitter or the receiver, or both, if enough knowledge is available about the system. In general, the receiver is optimized in order to improve the mean-square error, output Signal-to-Noise Ratio (SNR), probability of error etc. This can be achieved with some improved designs of receiver filter and decision unit. In this work, we study the receiver when the channel characteristics are unknown at the receiver end. Our approach is to minimize the mean-square error, thus to reduce the effect of both intersymbol interference and noise.

II.2 Intersymbol Interference and White Noise

The additive noise encountered by the system causes errors in the detection. The other concern for the designer of the optimal receiver is intersymbol interference. Using,

$$r_k = \sum_n a_n h_{k-n} + n_k, \tag{2.9}$$

then (2.8) can be written as,

$$r_k = a_k h_0 + \sum_{n \neq k} a_n h_{k-n} + n_k. \tag{2.10}$$

The desired output is the $a_k h_0$ term in the above equation, this corresponds to the r_k received sample. However, the rest of the terms are undesired components. These represent the noise and interference due to the tails of the system impulse response.

This interference due to past and future samples of $h(t)$ at the sampler output are referred to as the Intersymbol Interference (ISI).

To eliminate the ISI, the Nyquist criterion can be applied, the derivation of which follows. For a desired response of an impulse, i.e. no ISI at the sampling instants,

$$h_n = \begin{cases} h_0 & n = 0; \\ 0 & otherwise. \end{cases}, \tag{2.11}$$

an equivalent condition is that

$$h(t)\sum_n \delta(t - nT) = h_0\delta(t), \tag{2.12}$$

where $\delta(t)$ is the delta function. Since $\sum_n \delta(t - nT)$ is a periodic function, it has a Fourier series representation as,

$$\sum_n \delta(t - nT) = \frac{1}{T}\sum_n \exp(j\frac{2\pi tn}{T}). \tag{2.13}$$

Applying this to (2.12),

$$h(t)\sum_n \exp(j\frac{2\pi tn}{T}) = Th_0\delta(t), \tag{2.14}$$

and taking the Fourier transform of both sides

$$\sum_n H(f - \frac{n}{T}) = Th_0. \tag{2.15}$$

The lefthand side of the above equation is a periodic function of f with period $1/T$. The first period is called the Nyquist equivalent of $H(f)$ which is designated as,

$$H_{eq}(f) = \sum_n H(f - \frac{n}{T}) \qquad |f| < \frac{1}{2T}. \tag{2.16}$$

It can easily be observed that for the elimination of intersymbol interferance $H_{eq}(f)$ should be flat. This amounts to the requirement that at each sampling instant all h_n's be zero except h_0.

CHAPTER III

OPTIMAL MINIMUM MEAN SQUARE ERROR EQUALIZATION

III.1 Structure of Optimum Receiving Filter

In this chapter, the structure of the receiver is discussed and an optimization analysis is carried out. The possible criteria to optimize the receiver are introduced, and one selected, namely minimization of the mean-square error.

For a receiver structure as in Figure 2.1, which has a receiving filter, a detector and a decision unit, Ericson proposed a model which performs at least as well as any other filter. He shows that the optimum linear filter can be decomposed into two parts, a matched filter and a periodic filter. The former is a filter of the same bandwidth as that of the channel, while the latter can be implemented as a transversal filter. Then

$$H_r(f) = \frac{H^*(f)}{\Phi_{nn}(f)} P(f) \tag{3.2}$$

for

$$H(f) = H_e(f) H_m(f)$$

and $P(f)$ is periodic with period $1/T$. $H_r(f)$, the receiver input filter performs at least as well as any other linear filter for the minimization of intersymbol interference, signal-to-noise ratio, and error probabilty criterion.

The periodic frequency response of $P(f)$ can be represented by an infinite analog transversal filter. Such a filter is shown in Fig. 3.1. Based on the above result, the receiver of a basic communication system can be shown as in Figure 3.2.

The term $H_m^*(f)/\Phi_{nm}(f)$ is the frequency response of the filter which is matched to the signal waveform. This structure can be summarized as follows: the matched filter maximizes the signal-to-noise ratio at the decision instant, while the transversal filter $P(f)$, reduces the intersymbol interference that still corrupts the signal in its input.

However, the above receiver model is impractical due to the following reasons; (i) An infinite length transversal filter cannot be realized. (ii) Since the channel characteristics are assumed to be unknown, each time a connection is made, it is impractical to realize a matched filter (or even when the same channel is used and the channel itself slowly changes in time).

In practice, only a cascade of a lowpass filter and a transversal filter is used. Another simplification in the implementation is to place the sampler in Figure 3.3 before the transversal filter (to keep the samples in digital form for use in the calculation of the optimum tap coefficients). This reduces the transversal filter to a shift register. The adaptation procedure can then be performed digitally. One more point is that the transversal filter can be used to minimize the intersymbol interference by forcing the overall response $H(f)$ to obey (2.14). This causes the Nyquist equivalent channel to be flat. The name equalizer is given for that reason. The final form of the suboptimal digital receiving end is summarized as in Figure 3.3.

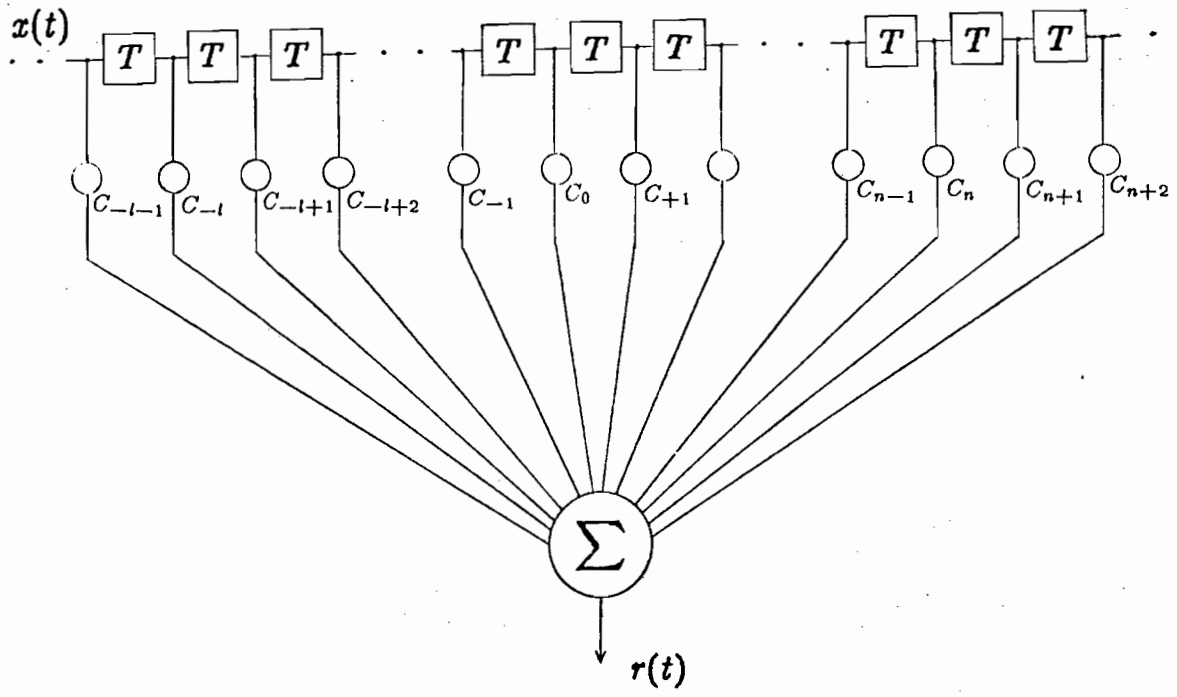

Figure 9.1 Infinite Transversal Filter.

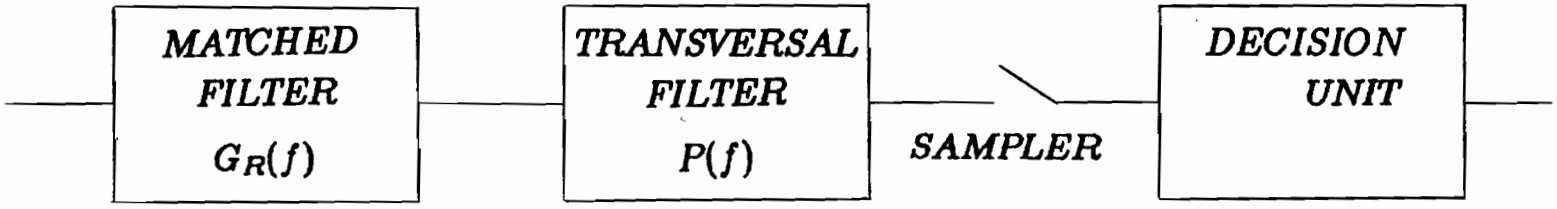

Figure 3.2 Basic Receiver.

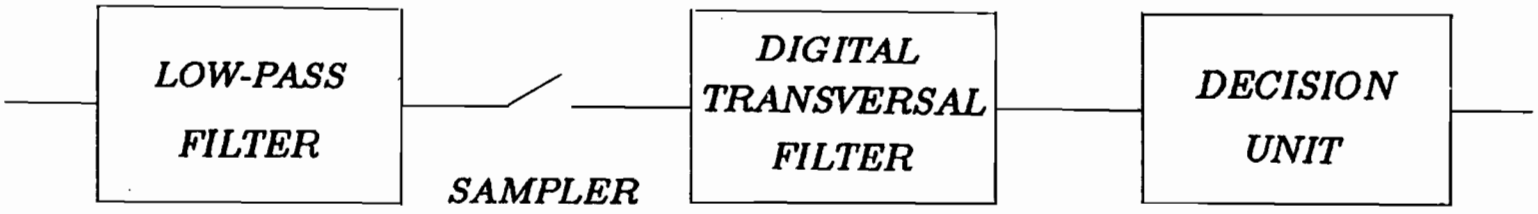

Figure 3.3 Suboptimal Receiving System.

III.2 Criteria for Optimal Receiver Design

To design the receiver, one must first come up with a receiver structure. Then, given this structure, the filter $H(f)$ can be optimized. But, due to intersymbol interference, there are several different optimization criteria. One of them is to try to minimize the error probabilty resulting from the noise and intersymbol interference, but this approach leads to quite intractable calculations. To obtain the solution, one has to solve a set of complicated nonlinear simultaneous equations. A much simpler approach, is to eliminate the intersymbol interference, and then minimize the error probability subject to some constraint. Maximizing the signal-to-noise ratio at the sampling instants can also be used as another optimization criterion. The equalization is achieved by finding a set of gains for the equalizer taps. These tap coefficients can be put in a vector form, (*)

$$\bar{C} = (c_{-N_1}, \ldots, c_0, \ldots, c_{N_2})^T, \tag{3.3}$$

where there are N_1 taps to the left, N_2 taps to the right of the reference tap (see Figure 3.4). The values of these taps are chosen so as to minimize the mean-square error between the output of the data source and output of the decision unit in the receiver. In the next section, the optimization problem is solved for a generalized equalizer in which the spacing between the taps is arbitrary. The special cases to be studied are derived from this model.

* $[.]^T$ is the transpose of the vector.

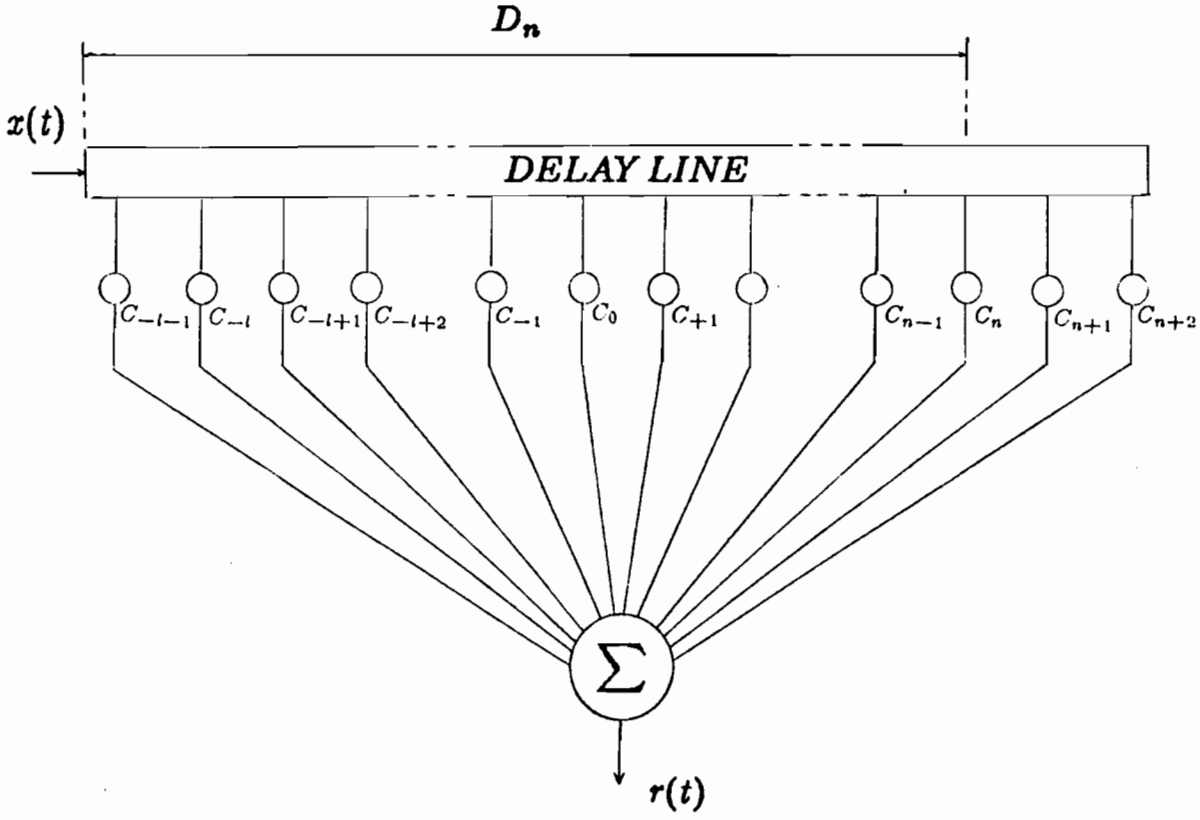

Figure 3.4 Generalized Equalizer.

III.3 Generalized Optimal Mean Square Error Equalizer

The generalized equalizer with arbitrary tap spacing is shown in Figure 3.4. Using an analog version of the equalizer (a tapped delay line) with a continuous signal at its output,

$$x(t) = \sum_n a_n \; h(t - nT) + n(t). \tag{3.4}$$

For arbitrary spacing, D_jT of tap spacings then, the output of the equalizer can be written as:

$$y(t) = \sum_j c_j \; x(t - D_jT). \tag{3.5}$$

The j^{th} tap has a delay of D_jT associated with itself. The above output is then sampled at symbol intervals. The output of the sampler feeds the following signal to the decision unit

$$y(kT + \tau) = \sum_j c_j \; x(kT - D_jT + \tau), \tag{3.6}$$

where τ is the sampling time offset with respect to source clock. Using the vector notation:

$$\bar{y} = \bar{C}^T \; \bar{x}_k \tag{3.7}$$

where: $\bar{C}$ is the vector of the tap coefficients;

$$\bar{x}_k^T \triangleq [..., x(kT - D_{-1}T), x(kT - D_0T), x(kT - D_1T), ...] \tag{3.8}$$

$$y_k \triangleq y(kT+\tau) \tag{3.9}$$

Let the desired response of the overall system be $f(t)$. For a desired output, $d(t)$,

$$\begin{aligned} d(t) &= f(t) * \sum_n a_n \delta(t-nT) \\ &= \sum_n a_n \ f(t-nT). \end{aligned} \tag{3.10}$$

Clearly, a special case occurs when $f(t)$ is equal to $\delta(t)$. The main reason for the presence of a general $f(t)$ term is to include partial response signalling. For partial response a correlation is introduced between the past and the present symbols. In this work we keep this term to be $\delta(t)$ and try to eliminate intersymbol interference due to the channel characteristics.

The samples of the desired signal at the output are,

$$\begin{aligned} d_k &\triangleq d(kT) \\ &= \sum_n a_n \ f(kT-nT), \end{aligned} \tag{3.11}$$

$$d_k = \overline{a}^T \overline{f}_k, \tag{3.12}$$

where

$$\overline{f}_k \triangleq [.., f[(k-1)T], f[kT], f[(k+1)T], ..]^T. \tag{3.13}$$

By definition the error is:

$$e_k \triangleq y_k - d_k. \tag{3.14}$$

Then the mean-square error is

$$\overline{|e_k|^2} = \overline{(y_k - d_k)\ (y_k^* - d_k^*)}. \tag{3.15}$$

The above expectation is over the sample space a_k. The block diagram for the generation of the error signal is shown in Figure 3.5.

The minimum mean-square error can be achieved for the particular setting of tap weights. The calculation for finding the optimal settings which lead to the following equation can be found in Appendix A.1.

$$\bar{C} = A^{-1}\bar{\alpha} \tag{3.16}$$

where A is an N by N channel autocovariance matrix whose elements are given by:

$$A_{i,j} = \overline{x^*(kT - D_iT + \tau)x(kT - D_jT + \tau)}, \tag{3.17}$$

and $\bar{\alpha}$ is the vector having the elements:

$$\alpha_j = \overline{d_k^* \; x(kT - D_jT + \tau)}. \tag{3.18}$$

Inserting the expression for $x(kT - D_iT + \tau)$ as given by,

$$x(kT - D_iT + \tau) = \sum_j a_j \; h(kT - D_jT + \tau) + n(kT - D_iT + \tau), \tag{3.19}$$

into the equations (3.17) and (3.18), we get an equation of the following form (see Appendix A.2)

$$A_{k,l} = \sum_i \sum_j \overline{a_i^* a_j} \; h^*[(k - D_k - i + \frac{\tau}{T})T] \; h^*[(k - D_l - j + \frac{\tau}{T})T], \tag{3.20}$$

$$\alpha_i = \sum_m \phi_{aa}(m)[\sum_n f(nT) \; h^*[(n - m - D_i + \frac{\tau}{T})T], \tag{3.21}$$

where:

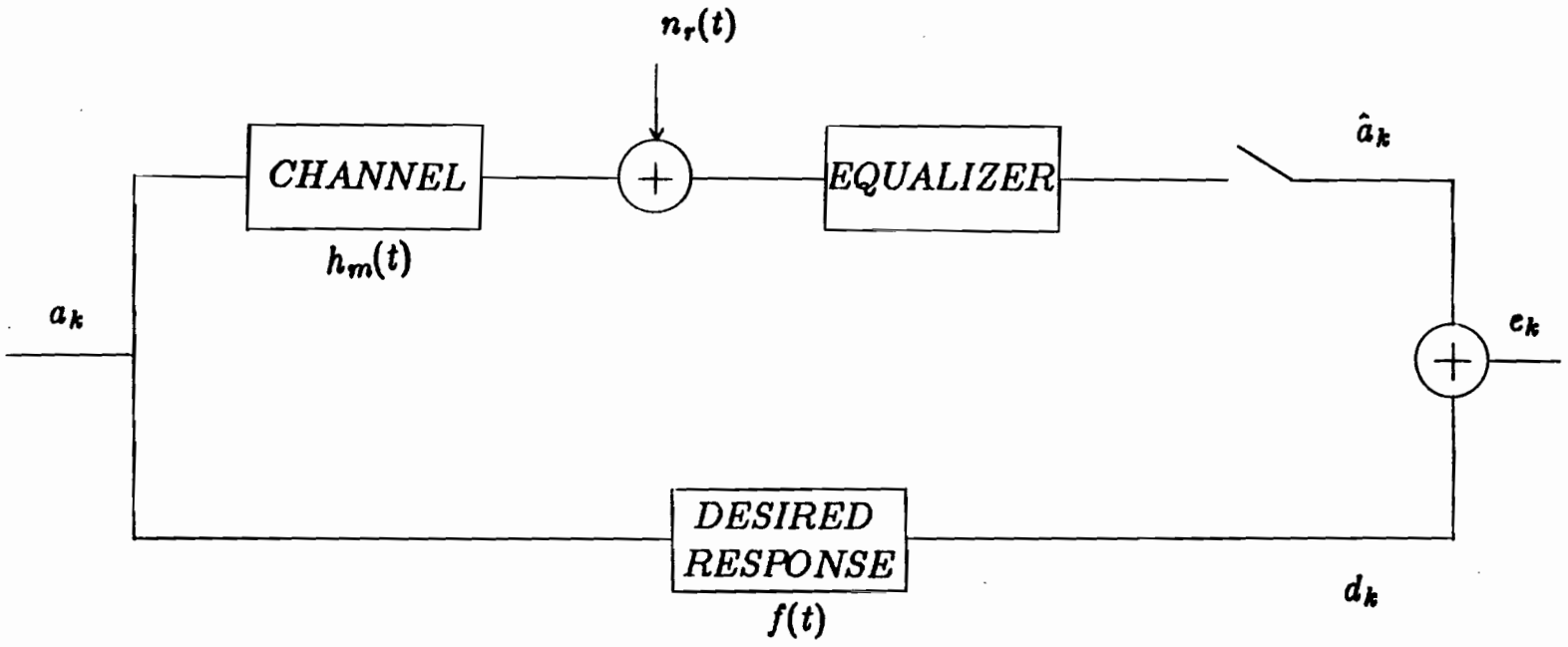

Figure 3.5 Generation of Error Signal.

$\phi_{aa}(.)$ is the autocovariance function of the data source,

$\phi_{nn}(.)$ is the autocovariance function of the noise,

$f(.)$ is the desired overall response.

In the conventional case, where the tap spacings are all T, i.e., $D_i = i$, and the data source is uncorrelated, with power σ_a^2 and the noise is white with power σ_n^2, we have:

$$\alpha_i = \sigma_a^2 \sum_n f^*(nT) h[(n - i + \frac{\tau}{T})T]. \tag{3.23}$$

The elements of the A matrix can also be written as follows

$$A_{k,l} = \sigma_a^2 \sum_n h^*[(n - \frac{\tau}{T})T] h[(n - \frac{\tau}{T})T + (i - j)T] \ ] + \sigma_n^2 . \delta_{i,j}, \tag{3.24}$$

With this final form of the matrix elements, it can easly be seen that the $(i,j)^{th}$ position in the matrix depends on $(i - j)$. A matrix which has this property is called Toeplitz and is a special case for the conventional equalizer. In general for D_i other than i, A is not Toeplitz.

A more general case is the one in which $D_i = i/n$, in this case there are n taps for each T second interval. The most important case for our purposes is when the taps are spaced by half the signalling interval. Using the transform relation,

$$h(t) = \int_{-\infty}^{+\infty} H(f) \ \exp(j2\pi ft) \ df,$$

to express the samples of $h(t)$ in the above equations for the A matrix elements, it can be shown that (3.20) and (3.21) can be written as (see Appendix A.3):

$$A_{k,l} = \frac{1}{T} \int_{-\frac{1}{2T}}^{+\frac{1}{2T}} H_{eq}^{k^*}(f) H_{eq}^{l} \ \Phi_{aa}(f) \ df + \Phi_{nn}[(D_k - D_l)T], \tag{3.25}$$

where

$$\Phi_{aa}(f) \triangleq \sum \phi(m) \ \exp(-2j\pi f m T),$$

and

$$H_{eq}^{k}(f) \triangleq \sum_{i} H(f + \frac{i}{T}) \exp[(-j2\pi(f + \frac{k}{T})].$$

For, the conventional case discussed earlier

$$A_{k,l} = \frac{1}{T} \int_{-\frac{1}{2T}}^{+\frac{1}{2T}} \Phi_{aa}(f) \ |H_{eq}(f)|^2 \exp(-j2\pi f(l-k)T) \ df \ + \ \sigma_n^2 \delta_{k,l}, \tag{3.27}$$

where $H_{eq}(f)$ is the Nyquist equivalent channel defined earlier (for $\tau = 0$) as:

$$H_{eq}(f) = \sum_{i} H(f + \frac{i}{T}) \exp(j\frac{2\pi\tau}{T} i).$$

By using Eq. (3.23) and the Fourier transform relations of $h(t)$ and $d(t)$ one can show that for the conventional case

$$\alpha_k = \frac{1}{T} \int_{-\frac{1}{2T}}^{+\frac{1}{2T}} H_{eq}^{*}(f) \ F_{eq}(f) \ \Phi_{aa}(f) \exp(-j2\pi f\tau) \exp(j2\pi f k T) \ df, \tag{3.28}$$

where $F_{eq}(f)$ is the Nyquist equivalent of the desired overall response. For the uniform case in which $D_i = i/2$ the elements of the autocovariance matrix can be written as

$$A_{k,l} = \frac{1}{T} \int_{-\frac{1}{2T}}^{+\frac{1}{2T}} \Phi_{aa}(f) \ |H_{eq}(f)|^2 \exp(-j2\pi f(l-k)\frac{T}{2}) \ df \ + \ \sigma_n^2 \delta_{k,l} \tag{3.29}$$

where k and l are even,

$$A_{k,l} = \frac{1}{T} \int_{-\frac{1}{2T}}^{+\frac{1}{2T}} \Phi_{aa}(f) \ |\hat{H}_{eq}(f)|^2 \exp(-j2\pi f(l-k)\frac{T}{2}) \ df + \ \sigma_n^2 \delta_{k,l} \tag{3.30}$$

where k and l are odd,

$$A_{k,l} = \frac{1}{T} \int_{-\frac{1}{2T}}^{+\frac{1}{2T}} \Phi_{aa}(f)\ H_{eq}(f)\ \hat{H}^{*}_{eq}(f) \exp(-j2\pi f(l-k)\frac{T}{2})\ df \tag{3.31}$$

where is k odd and l is even, and

$$A_{k,l} = \frac{1}{T} \int_{-\frac{1}{2T}}^{+\frac{1}{2T}} \Phi_{aa}(f)\ H_{eq}{}^{*}(f)\ \hat{H}_{eq}(f) \exp(-j2\pi f(l-k)\frac{T}{2})\ df \tag{3.32}$$

where is k even and l is odd, and

$$\hat{H}_{eq}(f) \triangleq \sum_{i} (-1)^{i} H(f + \frac{i}{T}) \exp(j2\pi \frac{\tau}{T}).$$

It is now apparent that A is no longer a Toeplitz matrix. By using Eq. (3.23) with $D_i = i/2$ and the transform relations for $f(t)$ and $h(t)$ it can be shown that the elements of the $\bar{\alpha}$ vector are given by

$$\alpha_k = \frac{1}{T} \int_{-\frac{1}{2T}}^{+\frac{1}{2T}} H^{*}_{eq}(f)\ F_{eq}(f)\ \Phi_{aa}(f) \exp(j2\pi f\tau) \exp(j2\pi k f\frac{T}{2})\ df \tag{3.33}$$

for even k, and

$$\alpha_k = \frac{1}{T} \int_{-\frac{1}{2T}}^{+\frac{1}{2T}} \hat{H}^{*}_{eq}(f)\ F_{eq}(f)\ \Phi_{aa}(f) \exp(j2\pi f\tau) \exp(j2\pi k f\frac{T}{2})\ df \tag{3.34}$$

for odd k.

This generalized equalizer analysis will serve as the basis for the analysis carried out in the rest of the thesis work. The studies on conventional equalizer, fractionally-spaced equalizer and hybrid equalizer will refer to this chapter, as special cases of the generalized equalizer. In the next chapter, we will introduce and discuss the properties of these equalizers.

CHAPTER IV

PROPERTIES of T, $T/2$-SPACED and HYBRID TRANSVERSAL EQUALIZERS

IV.1 Implementation of Equalizers

In the previous sections we have mentioned that equalizers are placed at the receiver end as decision-directed adaptive receivers. This chapter discusses the theory and the implementation techniques as well as the properties of adaptive equalizers.

For optimum equalization, one has to find the set of tap coefficients to reduce intersymbol interference and noise. The solution (3.16) involves the inversion of the $N \times N$ A matrix, where N, the total number of taps may be quite large. Iterative methods for solving Eqn. (3.16) will be discussed in the next chapter.

The hardware implementation of the adaptive equalizers can be classified into the following categories: analog, hardwired digital and programmable digital.

Early implementations used analog tapped delay lines, made up of inductor-capacitor (LC) and switched ladder attenuators as tap gains. Field-effect transistors later replaced the switched attenuators. As the technology became available, digi-

tal implementations were introduced, offering reduced size and increased accuracy. More recently, large-scaled integrated (LSI) analog implementations based on the charge-coupled device (CCD) technology renewed the interests in analog techniques. In this technique the sampled input waveform is stored and transferred as continuous-valued charge packets. The variable tap gains are stored in digital form, and the multiplication of the tap gains and the samples are done using a multiplying digital-to-analog converter. This method is still to be implemented, but it has significant potential in applications where the symbol rates are high enough to make the digital versions impractical or very costly.

The other class, namely the hardwired digital technology which was the most commonly used during the past decade. The input signal is used in sampled and digitized form, suitable for storing in the registers. The tap gains were stored in the digital shift registers as well. The formation and accumulation of products takes place in logic circuits connected to perform digital arithmetic.

The most recent advance in the field is the application of programmable digital signal processors. In this type of implementation the equalization function is performed in a series of steps or instructions in a microprocessor or a digital computation structure specially built to efficiently perform the type of digital arithmetic required. The same hardware can then be time-shared to perform functions such as filtering, modulation and demodulation in a modem. The greatest advantage of this technology is that it is flexible, and permits sophisticated equalizer structures and training procedures to be implemented with ease.

IV.2 Properties of T-spaced Equalizer

IV.2.1 The Autocovariance Matrix and its Eigenvalues

In this section we will first find the expressions for the eigenvalues and eigenvectors for the autocovariance matrix of an infinite T-spaced equalizer. As discussed earlier (from Eqn. (3.27)):

$$A_{k,l} = \frac{1}{T} \int_{-\frac{1}{2T}}^{+\frac{1}{2T}} \Phi_{aa}(f)\ |H_{eq}(f)|^2 \exp(-j2\pi f(l-k)T)\ df + \sigma_n^2 \delta_{k,l}, \tag{4.1}$$

where $H_{eq}(f)$ is the Nyquist equivalent channel. For a general row, s, of the Toeplitz A matrix, we have (for $\sigma_n^2 = 0$):

$$\begin{aligned} \sum_l A_{s,l} \exp(j2\pi\lambda Tl) &= \sum_l \frac{1}{T} \int_{-\frac{1}{2T}}^{+\frac{1}{2T}} |H_{eq}(f)|^2 \Phi_{aa}(f) \exp(j2\pi f s T) \exp(-j2\pi(f-\lambda)lT)\ df \\ &= \frac{1}{T} \int_{-\frac{1}{2T}}^{+\frac{1}{2T}} |H_{eq}(f)|^2 \Phi_{aa}(f) \exp(j2\pi f s T) \sum_l \exp(-j2\pi(f-\lambda)lT)\ df. \end{aligned} \tag{4.2}$$

Now, we have vectors of which having components $\exp(j2\pi f s T)$. Thus, these are the eigenvectors of the A matrix. Moreover the corresponding eigenvalues are:

$$|H_{eq}(f)|^2 \Phi_{aa}(f) \exp(j2\pi f s T). \tag{4.3}$$

In this section we will state a theorem which will be relevant in the latter sections.

Theorem 1:

The eigenvalues of the system autocovariance matrix are bounded by maximum value M and the minimum value m of $|Heq(f)|^2$; $(\sigma_n^2 = 0)$.

$$m \leq \lambda_A \leq M. \tag{4.4}$$

See Appendix (A.4) for the proof of this theorem. Therefore, the larger the spread of the eigenvalues, the farther the Nyquist equivalent response of the channel is from being flat. This fact is very much related to the convergence time of the taps, as will discussed in the following chapter.

IV.2.2 The Frequency Response of the Equalizer

In the previous chapter we have shown that, the optimal tap gains can be determined from

$$A\ \bar{C} = \bar{\alpha}. \tag{4.5}$$

We can write the same equation also in the following form

$$\sum_k \sum_l A_{k,l} C_l \exp(-j2\pi\lambda kT) = \sum_k \alpha_k \exp(-j2\pi\lambda kT). \tag{4.6}$$

Substituting equations (3.27) and (3.28) in the above equation, assuming white noise present one can show that the first period of the periodic frequency response of an infinite T-spaced equalizer is given by

$$C(f) = \frac{\Phi_{aa}(f)\ F_{eq}(f)\ H_{eq}(f)\exp(j2\pi f\tau)}{\Phi_{aa}(f)\ |H_{eq}(f)|^2 + \sigma_n^2} \qquad |f| < \frac{1}{2T}. \tag{4.7a}$$

In the noiseless case, the above equation simplifies to

$$C(f) = \frac{F_{eq}(f)}{H_{eq}(F)} \exp(j2\pi f\tau) \qquad |f| < \frac{1}{2T}. \tag{4.7b}$$

It is apparent that any zero of $H_{eq}(f)$ within the Nyquist range will be a pole of $C(f)$. One very important phenomenon occurs when dips in amplitude occur in $H_{eq}(f)$. Note that although $H(f)$ may have no zeroes (or near zeroes) in $|f| < 1/2T$, $H_{eq}(f)$ may have zeroes because of the superposition of terms such as $H(f+i/T)\exp(j2\pi\tau i/T)$ in $H_{eq}(f)$. Note that sampling phase affects $H_{eq}(f)$: certain choices of τ can cause dips in $H_{eq}(f)$, resulting in a $C(f)$ which has large peaks. This in turn can give rise to very large values of tap coefficients which may cause problems in practical realizations. These large values of tap gains may cause severe noise enhancement at certain frequencies, increasing the probability of error. Thus, there should be a good means of sampling phase control in the system in order to overcome the problem of sampling phase dependence on the performance of a T-spaced equalizer.

IV.2.3 The Minimum Mean Square Error of an Infinite T-Spaced Equalizer

From the previous chapter, we have the following equation for the minimum mean square error,

$$\overline{|e|}^2_{min} = \overline{|d|^2} - \bar{\alpha}^H \bar{C}_{opt}$$

the first term can be expressed as

$$\overline{|d|^2} = \frac{1}{T} \int_{-\frac{1}{2T}}^{+\frac{1}{2T}} |F_{eq}(f)|^2 \Phi_{aa}(f)\, df, \tag{4.8b}$$

and the second term, as

$$\bar{\alpha}\bar{C}_{opt} = \frac{1}{T}\int_{-\frac{1}{2T}}^{+\frac{1}{2T}} H_{eq}(f)F^*_{eq}(f)\exp(2j\pi f\tau)\Phi_{aa}(f)C(f)\ df. \tag{4.9}$$

Taking the difference of equations (4.7) and (4.8) we arrive at,

$$\overline{|e|}^2_{min} = \frac{\sigma_n^2}{T}\int_{-\frac{1}{2T}}^{+\frac{1}{2T}} \frac{|F_{eq}(f)|^2\Phi_{aa}(f)}{|H_{eq}(f)|^2\Phi_{aa}(f)+\sigma_n^2}\ df \tag{4.10}$$

For the noiseless case, the above equation shows that an infinite length optimum equalizer gives zero mean-square error. It can be easily observed that once there is noise introduced by the system, its significance is highly dependent on τ, the sampling phase which is in the $|H_{eq}(f)|^2$ term. For some values of τ, a null or near null may be introduced in $H_{eq}(f)$ within the Nyquist range at some frequencies and by Eq.(4.10) this may cause a large value for the integrand and thus a large minimum mean-square error.

IV.3 Properties of $T/2$-spaced Equalizer.

IV.3.1 The frequency Response of the $T/2$ Equalizer

We will start from the same expression for the optimal coefficients, namely,

$$A\ \bar{C} = \bar{\alpha}$$

where the elements of A matrix, and $\bar{\alpha}$ vector are given by Eq.(3.29) to (3.34). We will make the following definitions in order to derive an expression for the infinite $T/2$ equalizer: Let $\{c_k\}$, $k = -\infty$ to $+\infty$ represent the gains of an infinite T-spaced equalizer, and let d_k for all k but $k = 0$, be the gains of additional taps inserted between the c_k's. Then the frequency response of the $T/2$-spaced equalizer is:

$$C(f) = c(f) + d(f), \tag{4.11}$$

where:

$$c(f) \triangleq \sum_k c_k \exp(j2\pi f 2k\frac{T}{2}), \tag{4.11a}$$

and:

$$d(f) \triangleq \sum_k d_k \exp(j2\pi f(2k+1)\frac{T}{2}). \tag{4.11b}$$

By using the same steps as in the previous analysis for the T-spaced case, we come up with (for $\hat{H}_{eq} = H_{eq}$) :

$$C(f) = \frac{2F_{eq}(f)\ \Phi_{aa}(f)\ H^*(f)\exp(j2\pi f\tau)}{\Phi_{aa}(f)\ [\ |\hat{H}_{eq}(f)|^2 + |H_{eq}(f)|^2\ ]\ +\ \sigma_n^2}. \tag{4.12}$$

The bracketed term in the denominator is equal to the folded power spectrum of the overall response only when $H(f)$ is bandlimited to $|f| < 1/2T$, then we may write,

$$C(f) = H^*(f)\exp(j2\pi f\tau)\ \frac{\Phi_{aa}(f)\ F_{eq}(f)}{\Phi_{aa}(f)\ [|H(f+1/T)|^2 + |H(f)|^2 + |H(f-1/T)|^2 + \sigma_n^2}. \tag{4.13}$$

The above equation can be viewed as in two parts, the first being the matched filter, and the other which combats the intersymbol interference. The matched filter is matched to the overall frequency response of the system up to the equalizer, for the maximization of signal-to-noise ratio at the sampling instants.

A comparison of the $C(f)$'s for the $T/2$ case and the conventional case indicates that, there can be no poles caused by the denominator of $C(f)$ within the Nyquist range by the sampler timing offset τ. In fact, the denominator of $C(f)$ does not depend on τ and can be expressed in terms of the folded power spectrum of the unequalized channel for systems bandlimited to $1/T$.

IV.3.2 The Autocovariance Matrix and its Eigenvalues

Just as in the conventional case one can show that the eigenvectors and the eigenvalues of an infinite $T/2$-spaced equalizer are given by [Qureshi and Forney, 1977]:

$$U(f) = [... \pm \hat{H}^*_{eq}(f)\exp(-j2\pi f\frac{T}{2}), H^*_{eq}(f),$$

$$\pm\hat{H}^*_{eq}(f)\exp(j2\pi f\frac{T}{2}), \pm H^*_{eq}(f)\exp(j2\pi fT), ...], \tag{4.14}$$

and the corresponding eigenvalues, when (+) holds;

$$\lambda(f) = |H_{eq}(f)|^2 + |\hat{H}_{eq}(f)|^2, \tag{4.15}$$

and when (-) holds;

$$\lambda(f) = 0. \tag{4.16}$$

For $H(f)$ bandlimited to $|f| < 1/2T$, $\lambda(f)$ can be expressed as the folded power spectrum, i.e.

$$\lambda(f) = \sum_i |H(f - \frac{i}{T})|^2, \tag{4.17}$$

and for $|f| < 1/T$,

$$\lambda(f) = |H(f - \frac{1}{T})|^2 + |H(f)|^2 + |H(f + \frac{1}{T})|^2. \tag{4.18}$$

We see that a constant folded power spectrum in the $T/2$ case has the same effect as a constant folded spectrum in the conventional case: in both cases it is possible, by a judicious choice of the step size to have the taps gains reach their optimal values in one iteration.

Here, once again we observe that the eigenvalues are not dependent on the sampling timing offset, r, whereas in the T-spaced equalizer the eigenvalue spread is subject to change with r. Therefore we should expect the convergence of the infinite length fractionally-spaced equalizer to be independent of sampler offset.

IV.3.3 The Minimum Mean Square Error of an Infinite T/2-Spaced Equalizer

In this section we will derive an expression for the minimum mean-square error for a $T/2$ equalizer. By applying the similar procedure for the T equalizer case, the mean-square error is given by:

$$\begin{aligned}\overline{|e|^2_{min}} &= \bar{\bar{v}}^H \bar{U}\ \bar{\bar{v}} - \bar{\bar{\alpha}}^H \bar{C} \\ &= \sum_i \sum_j \overline{v_i^* v_j}\ u_i^* u_j - \sum_{even\ k} \alpha_i c_{i\ opt} - \sum_{odd\ k} \alpha_k d_{k\ opt},\end{aligned} \tag{4.19}$$

can be expressed as:

$$\overline{|e|^2}_{min} = \frac{\sigma_n^2}{T} \int_{-\frac{1}{2T}}^{+\frac{1}{2T}} \frac{|F_{eq}(f)|^2 \Phi_{aa}(f)}{\Phi_{aa}(f)\ [|\hat{H}_{eq}(f)|^2 + |H_{eq}(f)|^2] + \sigma_n^2}\ df. \tag{4.20}$$

It is seen here that mean-square error is not influenced by the sampling offset, r. A comparison of the mean-square error expressions of the equalizers shows that,

$$\overline{|e_{min\ \frac{T}{2}}|^2} \leq \overline{|e_{min\ T}|^2}$$

i.e. the $T/2$ equalizer performs better than the conventional case. It is also independent of r. The simulation results in this thesis, as well as in [Qureshi and Forney, 1977], [Ungerboeck, 1972] and [Ungerboeck, 1976] show these results clearly.

IV.4 Properties of HTE.

A hybrid type of equalizer was first introduced in [Nattiv and Kabal, 1980]. In their work they have defined the Hybrid Type Equalizer (HTE) as a T-spaced equalizer with some additional intermediate taps inserted around the reference tap. As these inserted taps had $T/2$ spacing with the adjacent taps, it is expected to have many of the benefits of a $T/2$ equalizer, and have a wider time span compared to a conventional equalizer with the same number of taps. This will enable the equalizer to eliminate the intersymbol interference due to the channels with long impulse responses. As additional taps are introduced to the T-spaced equalizer, the hybrid equalizer will resemble that of a pure $T/2$-equalizer. With the proper placement of taps it is also expected that the hybrid type equalizer will avoid nulls, or near nulls in the Nyquist range.

It will be shown in a later chapter that, the number of taps are related to the final mean-square error. In other words, minimum achievable mean-square error in steady-state is dependent on the number of taps, i.e. for larger N, beyond a certain value, the mean-square error will be slightly larger due to the adaptation fluctuations introduced by each tap. A hybrid equalizer reduces the complexity, as well as using less number of taps the excess mean-square error term is minimized. It is expected that the hybrid equalizer will be advantageous for both of these reasons.

In the following sections a summary of the work carried out by Nattiv [Nattiv, and Kabal, 1980] will be presented.

IV.4.1 The Optimal HTE

In the approach used to study the hybrid type equalizer, Nattiv considered the overall system to be made up of a T-spaced, and a $T/2$-spaced part. In other words

the equalizer has been split into three sections, ones having T and the other having $T/2$ spacing. An example with the partitioning of three is shown in the following figure (Figure 4.1). From this approach we have,

$$y_k = y_{k1} + y_{k2} + y_{k3}, \tag{4.21}$$

where:

$$y_{k1} = \sum_{i=-N_0}^{-N_1} c_i x_{k-i} \triangleq \bar{c}^T \bar{x}_k \tag{4.22}$$

$$y_{k2} = \sum_{i=-2N_1+1}^{2N_2} d_i x_{k-i} \triangleq \bar{d}^T \bar{x}_{k-d_1} \tag{4.23}$$

$$y_{k3} = \sum_{i=N_2+1}^{N_3} e_i x_{k-i} \triangleq \bar{e}^T \bar{x}_{k-d_1-d_2} \tag{4.24}$$

For this configuration the desired output can again be defined as,

$$d_k = \bar{a}_k^T \bar{f}_k,$$

where f_k are the samples of the overall impulse response. The mean-square error is,

$$\overline{|e_k|^2} = \overline{(y^*_k - \bar{a}^H \bar{f}_k^*)(y_k - \bar{a}^T \bar{f}_k)} \tag{4.25}$$

Inserting the equations (4.31) to (4.33) into the mean-square error expression (i.e. Eq.(4.34)), and differentiating the final form with respect to the tap coefficients, c_k, d_k, and e_k one obtains the following set of equations for the optimum hybrid equalizer,

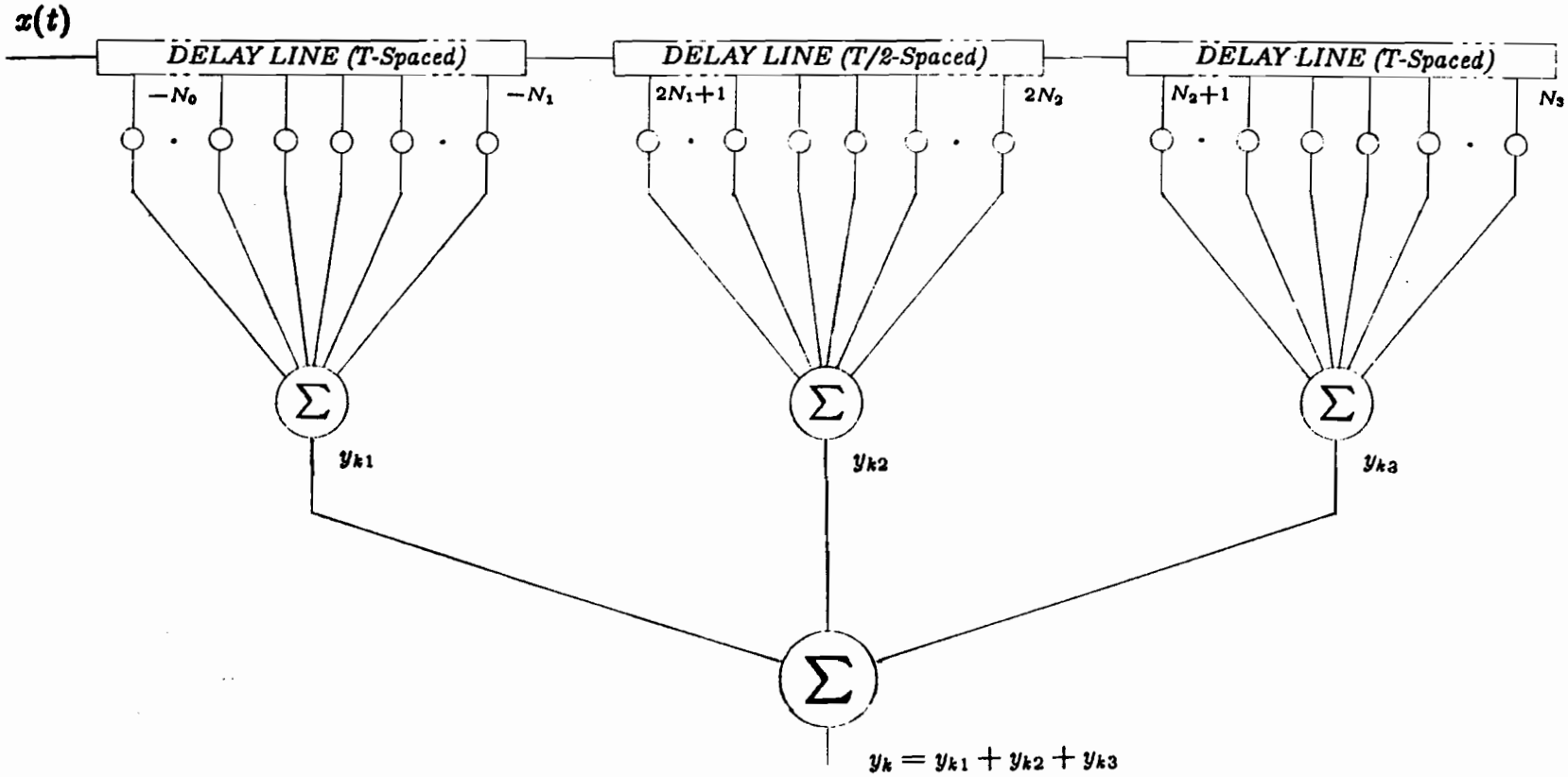

Figure 4.1 Hybrid Transversal Equalizer Model.

$$\begin{bmatrix} A_1 & B & W \\ B^H & A_2 & V \\ W^H & V^H & A_3 \end{bmatrix} \begin{bmatrix} \bar{c} \\ \bar{d} \\ \bar{e} \end{bmatrix} = \begin{bmatrix} \bar{\alpha}_1 \\ \bar{\alpha}_2 \\ \bar{\alpha}_3 \end{bmatrix}$$

The elements of the above matrix can be identified simply from the square error term, which are the auto- or the cross-correlation terms of the subsections.

The most important result is that the autocovariance matrix of the hybrid transversal equalizer can be derived from the matrix of $T/2$ case by deleting those rows and columns which are not used in the hybrid model. The similar manupulation also holds for the $\bar{\alpha}$ vector of the above equation.

For the frequency response of the hybrid transversal equalizer the equations are very complicated, and no compact form can be reached for practical purposes. However, the resulting equations show that as the number of additional taps are increased, the properties of the hybrid equalizer gets closer and closer to that of $T/2$-spaced equalizer.

In the next chapter we will introduce the convergence phenomenon, as well as some algorithms used for the adaptive equalizers. Then, we focus on the mean-square-algorithm, and discuss the convergence properties of the equalizer types discussed above.

CHAPTER V

CONVERGENCE PROPERTIES of the TRANSVERSAL EQUALIZERS

V.1 The Recursive Algorithms for Computing the Tap Gains

In this chapter we will introduce some of the techniques by which the tap coefficients are adjusted, and then analyse the steepest descent algorithm. In the rest of the chapter we will analyse the rate of convergence of the conventional equalizer and discuss for the fractionally spaced and hybrid equalizer cases.

The adaptation of the transversal filter to the channel response and the source signal is realized at the receiver by an iterative procedure to adjust the tap weights. The general adaptation method can be modelled by:

$$\bar{C}_{k+1} = \bar{C}_k - \bar{S}_k \tag{5.1}$$

where the $\bar{S}_k$ is a vector of tap gain increments. There are various algorithms that achieve adaptation. Many transversal filter equalizer update algorithms are based

on the steepest descent, or gradient technique, which minimizes the mean-square error between the equalizer output and the transmitted data symbols, given by (3.15);

$$\overline{|e_k|^2} = \overline{(y_k - d_k)(y^*{}_k - d^*{}_k)} \tag{5.2}$$

One algorithm invokes the minimization of least square the objective of which is to determine the coefficient vector which minimizes the weighted sum of the squared errors of past received signal vectors [Mueller, 1981], in other words it minimizes

$$\sum \lambda_{n-k} |d_k - \bar{C}^*_n \ \bar{x}_k|^2. \tag{5.3}$$

Setting the derivative of the above equation to equal to zero yields the discrete time Wiener-Hopf equation,

$$A_n \ \bar{C}_n = \bar{\alpha}_n \tag{5.4}$$

in the iterative form,

$$\begin{aligned} A_n &= \sum_k \lambda_{k-n} \bar{x}_n \ \bar{x}^*{}_n + \lambda_n \Delta I \\ &= \lambda \ A_{n-1} + \bar{x}_n \ \bar{x}^*{}_n \end{aligned} \tag{5.5}$$

and

$$\bar{\alpha}_n = \lambda \bar{\alpha}_{n-1} + \bar{x}_n \ d^*{}_n \tag{5.6}$$

A positive definite identity matrix ΔI is included to ensure positive definiteness of $A = n$ for all n.

Since the above two equations can be written recursively, the updated coefficient can be found iteratively as follows,

$$\bar{C}_n = \bar{C}_{n-1} + g_n \vec{e}_n \tag{5.7}$$

where g_n is the Kalman gain defined as

$$g_n = A_n^{-1} \bar{x}_n \tag{5.8}$$

This form leads to the Kalman, the fast Kalman, and the adaptive lattice algorithms where in all cases the same cost function is minimized. The difference is in the manner and the complexity with which it is achieved. [Mueller, 1981]

In their work O.S. Kosovych and R.L. Pickholtz [9] proposed a new algorithm to improve the convergence rate, namely overrelaxation iterative technique. Where their method determines the coefficient value for all i, at the $(k+1)^{st}$ iteration acording to

$$c_{i\,(k+1)} = c_{i\,(k)} - \frac{w}{a_{ii}}\left[\sum_{j=-N}^{i-1} a_{ij}\ c_{j\,(k+1)} + \sum_{j=i}^{N} a_{ij} c_{j\,(k)} - g_i\right] \tag{5.9}$$

where w is the relaxation factor. In matrix form we have,

$$\bar{C}_{k+1} = \bar{C}_k - w(D - wE)^{-1}(A\bar{C}_k - g) \tag{5.10}$$

where E and D are the diagonal and strictly lower triangular matrices. Here the inverse of the A matrix is never computed if the above equation is used (5.9). All of the coefficients are updated prior to the reception of the next training pulse. This is a departure from gradient techniques since they use only the previous values.

As another example, the works carried out by T.J. Schonfeld and M. Schwartz, minimized the mean-square error by using variable step sizes after a specified number of iterations. The so called First-Order and Second-Order algorithms use a optimally determined step size in order to achieve minimum mean-square error.

These and other papers on the various algorithm on the convergence of adaptive equalizers can be found in the references [16] to [22]. In the following section the steepest descent algorithm will be studied using a constant step size parameter.

V.2 The Steepest Descent Algorithm

This section concentrate on the steepest descent technique to solve Equation (3.15) iteratively to find the optimal tap values. The convergence and the stability of the method will be discussed.

V.2.1 Performance Surface

The adjustment algorithm attempts to find the minimum of the mean-square error as a function of the tap weights. First, one begins by choosing an initial set of values for the set $\{c_n\}$ of tap gains. The gradient vector is measured, and the next guess is obtained from the present state of weights by making a change in the tap vector in the direction of the negative of the gradient vector (in the opposite direction of the gradient vector). If the mean error square is reduced with each change in the weight vector, the process will converge to a stationary point regardless of the initial choice.

In Figure 5.1a view of a two-dimensional (two tap) quadratic performance surface is shown. The mean-square error is shown as along the z-axis and the other coordinates are the two tap coefficients. The ellipses in the figures correspond contours of constant mean-square error, spaced at equal increments. The gradient must be orthogonal to these contours everywhere on the surface. In the following figure (Figure 5.1a) the series of small steps of the tap coefficients incremented

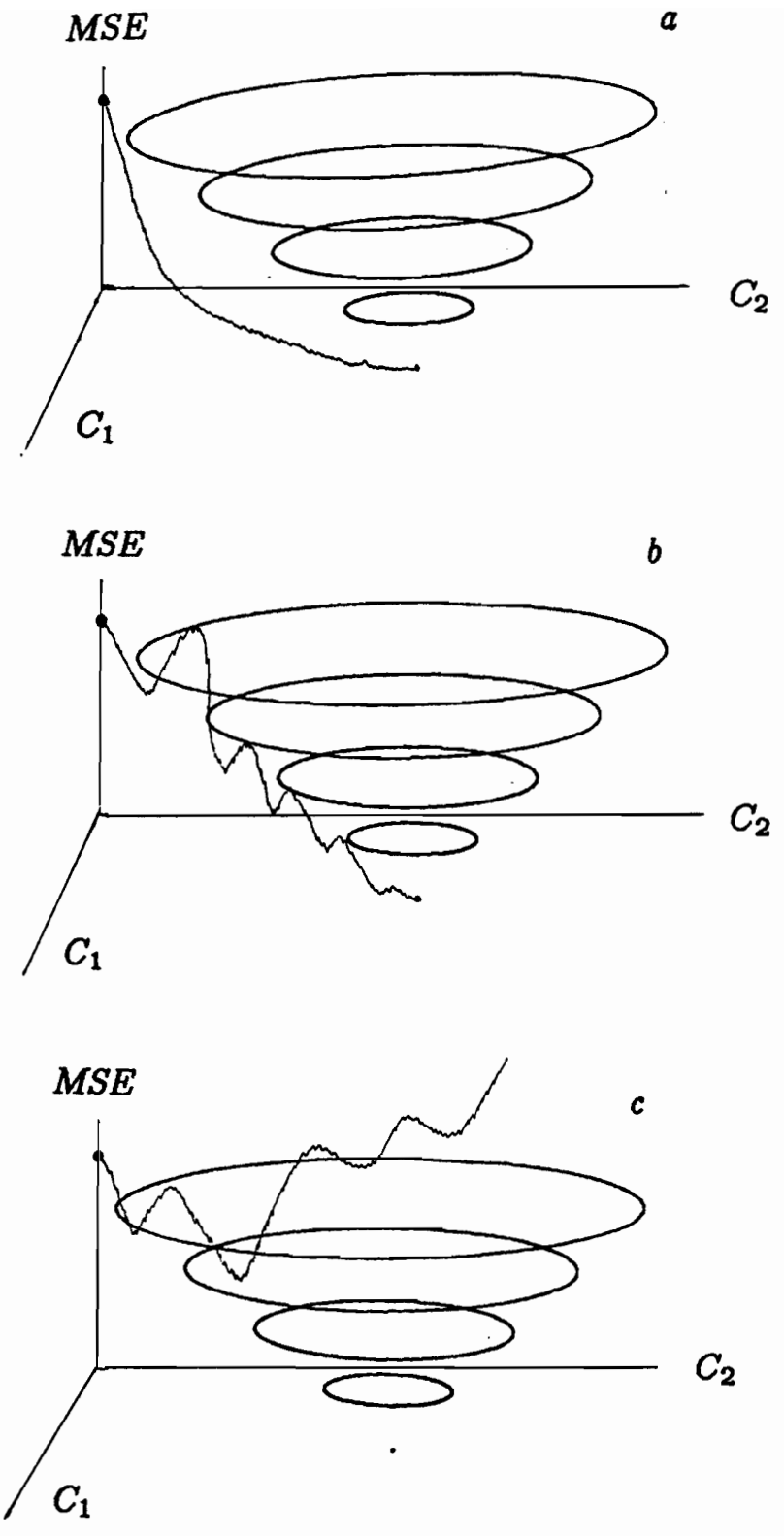

Figure 5.1 Steepest Descent Method.
a- Overdamped case
b- Underdamped case
c- Unstable case

by the discussed algorithm is shown, where the initial point is picked up for zero tap weights, and the small increments form a smooth curve. Figure 5.1b is a similar plot for a larger step size where convergence is more oscillatory, where as in Figure 5.1c a much larger step size is used, the stability of the equalizer is lost (stability criteria will be discussed later in the chapter). From the starting point, each step is taken normal to the error contour. It will be shown later that the weights undergo goemetric transients in converging towards the surface minimum.

From the above discussion we can set the following equation as a different form of equation (5.1),

$$\bar{C}_{k+1} = \bar{C}_k + s_k \bar{g}_k \tag{5.11}$$

where s_k is a parameter controlling the step size and $\bar{g}_k$ is the gradient vector,

$$\bar{g}_k = E|\frac{\partial e_k^2}{\partial C_k}| \tag{5.12}$$

where

$$e_k = d_k - y_k \tag{5.13}$$

Now the tap coefficient adjusment algorithm is of the form,

$$\bar{C}_{k+1} = \bar{C}_k + \Delta_k E[e_k r_k] \tag{5.14}$$

Which can also be written as

$$\bar{C}_{k+1} = \bar{C}_k + \Delta_k (A\bar{C}_k - \bar{\alpha}) \tag{5.15}$$

where Δ_k is the step size parameter (equal to $2\varepsilon_k$), A is the correlation matrix of the input sequence (on the assumption of r_k and d_k are stationary sequences). The solution is

$$\bar{C}_{opt} = A^{-1}\bar{\alpha}. \tag{5.16}$$

The conditions for convergence of the taps can be derived easily after the following coordinate transformation.

V.2.2 Coordinate Transformation

In order to decouple the tap coefficient adjusments we will define the transformation,

$$\bar{C}' \triangleq P\ \bar{C} \tag{5.17}$$

where P is an orthonormal matrix which diagonalizes A. This transformation is equivalent to a rotation of the coordinate system,

$$A = P^{-1}\Lambda\ P \tag{5.18}$$

and Λ is the diagonal matrix of the eigenvalues of λ_j of A . Then,

$$\bar{C}'_{k+1} = \bar{C}_k - \Delta_k[\Lambda\bar{C}'_k - P\bar{\alpha}] \tag{5.19}$$

In Figure 5.2 a feedback model for this adjusment algorithm is shown. The optimum decoupled weight vector can be written as,

$$\bar{C}'_{opt} = \Lambda^{-1}P\bar{\alpha} \tag{5.20}$$

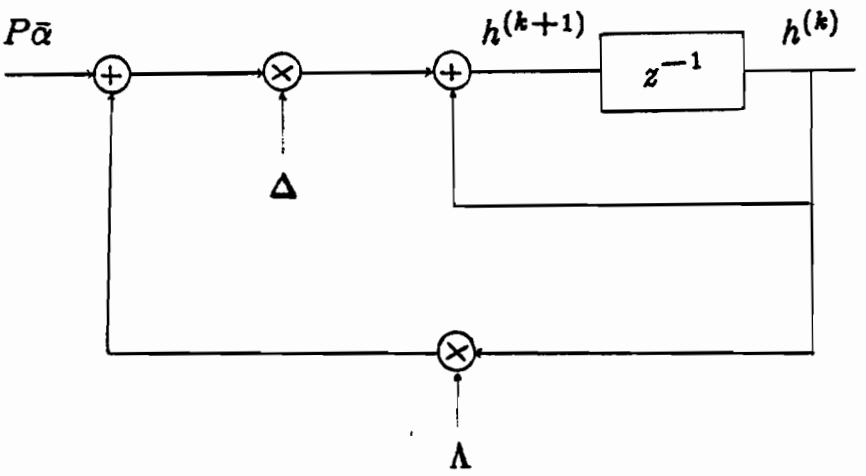

Figure 5.2 Feedback Model for the Tap Coefficient Adjusment.

We will also define the tap coefficient error as,

$$\bar{h_k} \triangleq \bar{C_k'} - \bar{C_{opt}'} \tag{5.21}$$

V.2.3 Convergence and Stability of h and C

From equation (A.I.3) which is repeated here,

$$\overline{|e|^2} = \bar{C}^H A \bar{C} - \bar{\alpha}^T \bar{C} - \bar{C}^H \bar{\alpha}^* + \overline{|d_k|^2} \tag{5.22}$$

we get

$$\overline{|e|^2} = \overline{|e_{opt}|^2} + \bar{h}_k^T A \ \bar{h_k}. \tag{5.23}$$

In the iterative form suitable for adaptive equalizer,

$$\bar{h}_{k+1} = \bar{h_k} - \Delta_k \Lambda e_k r_k. \tag{5.24}$$

Defining

$$e_k \triangleq \bar{C}_{k\ opt}^T \ r_k - d_k, \tag{5.45}$$

we have,

$$e_k = e_{k\ opt} + \bar{h}_k^T \ r_k. \tag{5.26}$$

Note that,

$$\overline{e_k r_k} = 0, \tag{5.27}$$

which leads to

$$\overline{|e|^2} = \overline{|e_{opt}|^2} + \Lambda \bar{h}_k. \tag{5.28}$$

We will also restrict ourselves to a constant step size i.e. $\Delta_k = \Delta$. This gives us for each j, $j = 1, ..., M$, the z-transform of the j'th tap weighting error as

$$H_j(z) = \frac{z\ h_j^0}{z - \Delta\lambda_j} \tag{5.29}$$

The limit as $k \to \infty$ of $|H_j(k)|$ is zero if and only if all of the poles of $H_j(z)$ are within the unit circle in the complex z-plane.

If

$$\lim_{k\to\infty} |h_{j(k)}| = 0 \tag{5.30}$$

then,

$$\lim_{k\to\infty} \bar{C}_k' = \bar{C}_{opt}' \tag{5.31}$$

The criteria for the convergence and the stability can be derived as follows. For the positive definite autocovariance matrix A, we have $\bar{u}^T A \bar{u} > 0$, for all $\bar{u}$. Then from Eq.(5.15) by subtracting $\bar{C}_{opt}$ from both sides

$$\begin{aligned} \overline{\Delta C}_{k+1} &= \overline{\Delta C}_k - \Delta A \overline{\Delta C}_k \\ &= (I - \Delta A)\overline{\Delta C}_k \end{aligned} \tag{5.32}$$

Making use of the coordinate transformation and the definition in Eq.(5.21),

$$\bar{h}_{k+1} = (I - \Delta\Lambda)\bar{h}_k \tag{5.33}$$

For each of the decoupled components

$$\overline{h_{i(k+1)}} = (1 - \Delta\lambda_i)\overline{h_{i(k)}} \qquad i = 1, ..., N \tag{5.34}$$

where λ_i is the ith eigenvalue of A. For convergence,

$$\overline{h_{i(k+1)}} < |1 - \Delta\lambda_i|\overline{h_{i(k)}} \tag{5.35}$$

for all k and i, which leads us to choose the step size acording to

$$|1 - \Delta\lambda_i| < 1. \tag{5.36}$$

Considering the maximum and the minimum values of the eigenvalues, and choosing a step size of,

$$\Delta = \frac{2}{\lambda_{A_{min}} + \lambda_{A_{max}}} \tag{5.37}$$

we get,

$$|1 - \Delta\lambda_{min}| = \frac{\lambda_{A_{max}} - \lambda_{A_{min}}}{\lambda_{A_{max}} + \lambda_{A_{min}}} < 1 \tag{5.38}$$

Therefore a step size in the proper range will lead to convergence of the mean tap values in the limit. Convergence in the mean does not depend on the number of taps. If the mean square convergence is considered, stability does depend on the number of taps[Mazo]. The convergence rate and stabilty is directly related to the choice of Δ. Relating this to the channel response, if the channel response is flat (the spread of the eigenvalues of the A matrix is small) the convergence will be fast.

V.3 Excess Mean-Square Error (e_Δ^2)

The measurement of noise in the recursive algorithm discussed above has a mean-square error value that is proportional to the step size parameter (Δ). The noise in the tap updating procedure due to the use of estimates rather than the true value of the gradient components causes random fluctuations in the tap gains about their optimal values. This leads to an increase in the mean-square error at the output of the receiver. Thus the steepest descent algorithm will converge to $e_{min}^2 + e_\Delta^2$, in the mean-square sense, where e_Δ^2 is the variance of the measurement noise.

The increase of MSE above the minimum achievable mean-square error due to the estimation noise has been named "excess mean-square error", [Widrow 1966]. Since the amplitude of the random fluctuations of the tap gains increase with an increase in the value of the step size, one has to be careful in choosing this parameter. A large step size will give a rapid adaptation, yet result in a higher excess MSE.

At any instant, using the set of $\{c_n\}$'s we can write,

$$e^2 = e_{min}^2 + (\bar{C} - \bar{C}_{opt})^H A\ (\bar{C} - \bar{C}_{opt}). \tag{5.39}$$

Using the coordinate transformations introduced earlier we have,

$$e^2 = e_{min}^2 + \sum_n \lambda_n\ |C_n' - C_{n\ opt}'|^2. \tag{5.40}$$

Where λ_n are the eigenvalues of A. The average of the increase in the MSE due to random fluctuations of the tap gains about their optimum values is given by;

$$e_\Delta^2 = \sum_n \lambda_n \overline{|C_n' - C_{n\ opt}'|^2} \tag{5.41}$$

Complete derivation of the computation of excess MSE using the signal and system parameters can be found in [Proakis and Miller, 1969]. The excess mean-square error is

$$e_{\Delta}^{2} = \frac{\Delta \ N \ e_{min}(\Phi_{aa} + \Phi_{nn})}{2} \tag{5.42}$$

Note that excess MSE is directly proportional to the number of taps and the step size. This result is collaborated in our simulation results presented in the next chapter.

CHAPTER VI

RESULTS

This chapter is devoted to simulation results. The comparison of the equalizers on the basis of their convergence properties follows the description of the methodology used. A study of the dependence of the step size and the number of equalizer taps is included.

VI.1 Description of the Simulation

The digital adaptive fractional-tap equalizer was simulated using a computer program. The program takes in the fraction of the symbol spacing, T/N, the overall system response (including the reference point), then the desired channel response (expressed in terms of the impulse response) is entered. The following transmission and equalizer characteristics are also entered: signal-to-noise ratio, size of input alphabet (only a binary alphabet is used for this particular study), number of taps, the subscript of reference tap (the program enables the user to change the particular hybrid tap configuration), and the proportionality constant used in incrementing the tap coefficients. Note that in order to keep the excess mean-square error approximately constant for configurations with different numbers of taps the step size is made to vary with number of taps. Also, the number of training and transmitting

symbols are specified.

With the above input values, the program computes the channel autocovariance matrix A and finds its eigenvalues. The optimum tap coefficients are calculated by solving the simultaneous equations of (3.16). The optimum MSE is found using the calculated optimum tap values. The tap coefficients are initialized (normally all zero or to the optimal values for checking purposes), the symbols and the noise components are generated using random number generating routines using the system time base to randomize the starting point. Every sample value is convolved with the overall system response, summed up with the noise component and passed through the equalizer. The output of the equalizer is decoded and the taps are updated using the steepest descent method. All the relevant data, such as the particular hybrid tap settings, eigenvalues, optimal tap values, and the errors at the output are stored for further analysis. Also, the output MSE after every ten iterations, the calculated MSE using the optimal tap coefficients, the convergence of the reference tap values, were utilized for plotting the necessary graphs.

Another program was also set up in order to find the optimal tap placings for the hybrid configuration, where all the possible hybrid configurations were generated, the optimum MSE was calculated, and for each additional tap, the minimum and maximum MSE's along with the particular tap configuration used were recorded. The results were used in choosing the placement of the additional taps.

The results displayed in this thesis are the outputs of the simulations using the two different channels which are selected from the papers [Ungerboeck],[Proakis]. In the rest of the chapter the channel responses will be referred as one (I) shown in Figure 6.1a, and the other (II) in Figure 6.1b. These channel responses have been interpolated in order to obtain the intermediate samples.

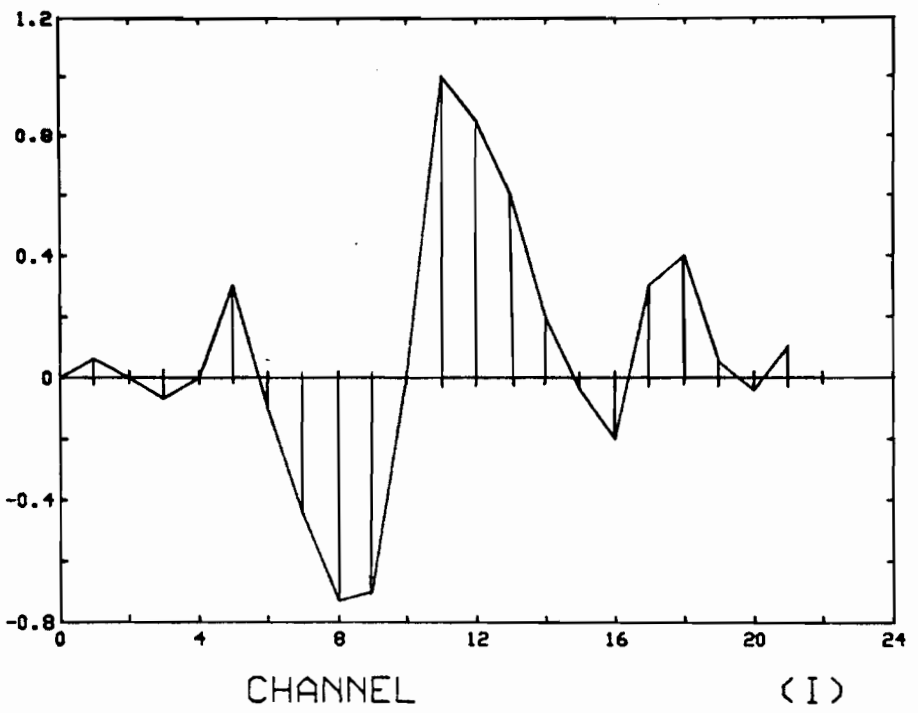

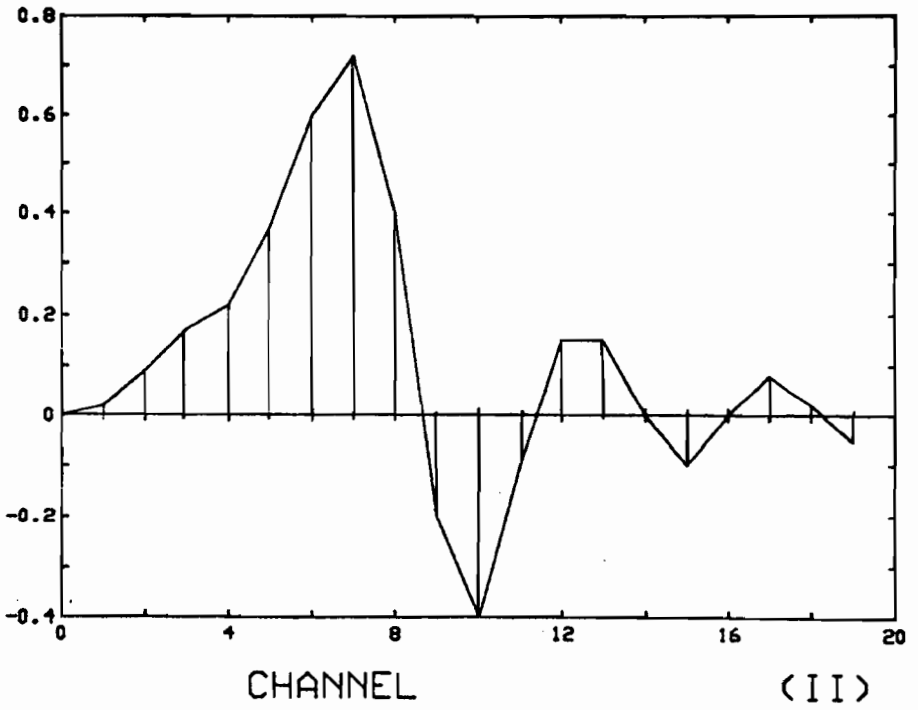

Figure 6.1 Sampled and Interpolated Impulse Responses of Simulated Transmission Channels.

VI.2 Comparison of the Equalizers

In Figure 6.2, the relation between the minimum achievable MSE obtained by directly solving (3.16) and the time span of the transversal equalizer is displayed for a $T/2$-spaced equalizer. One should notice that the practical adaptive equalizers have a higher MSE because of the excess mean-square error due to the noisy estimates in the tap updating algorithm. This excess men-square error is a function of the step size parameter and the number of taps. We shall discuss these two points later in this chapter. A similar plot was obtained for channel (II). These results show that an equalizer time span of $10T$ (20 taps) gives good results for both channels (I) and (II) .

When different number of additional taps are inserted between the taps of the T-spaced equalizer, it has been observed that the particular placement and the number of additional taps play a considerable role in the minimum MSE. The best and the worst MSE limits for every combination of the same number of additional taps were calculated, and a plot is obtained for an equalizer spanning $10T$ with zero to ten additional taps. Although it seems that every additional tap reduces the MSE, it should be apparent that the best placement of the additional taps is a major concern. Since in most practical applications this information is not available, a reasonable conjecture is that additional taps should be placed around the reference tap. To test this, we have calculated the mean-square error when the additional taps were clustered around the reference tap. In Figure 6.3, these results are plotted for channels (I) and (II) respectively. The optimum and worst case tap placements are given in Tables 1 and 2. It can easily be observed that the mid-taps are very good approximations for the optimal hybrid equalizer configurations for both channels. Therefore placing the additional taps around the reference tap seems to be a good choice.

Channel (I) Number of Additional Taps	MSE (in dB)	Tap Placements (*) (Hybrid T/2 taps)
1	Best MSE= -47.4	0 0 0 0 1 0 0 0 0 0
	Mid Tap MSE= -47.4	0 0 0 0 1 0 0 0 0 0
	Worst MSE= -35.3	0 0 0 0 0 0 0 0 0 1
2	Best MSE= -60.4	0 0 1 1 0 0 0 0 0 0
	Mid Tap MSE= -55.0	0 0 0 0 1 1 0 0 0 0
	Worst MSE= -35.5	1 0 0 0 0 0 0 0 0 1
3	Best MSE= -65.3	0 1 1 0 0 0 1 0 0 0
	Mid Tap MSE= -59.2	0 0 0 1 1 1 0 0 0 0
	Worst MSE= -37.8	1 1 0 0 0 0 0 0 0 1
4	Best MSE= -69.0	0 1 1 1 0 0 1 0 0 0
	Mid Tap MSE= -60.1	0 0 0 1 1 1 1 0 0 0
	Worst MSE= -39.7	1 1 0 1 0 0 0 0 0 1
5	Best MSE= -71.2	0 1 1 1 1 0 1 0 0 0
	Mid Tap MSE= -66.6	0 0 1 1 1 1 1 0 0 0
	Worst MSE= -41.3	1 1 0 1 0 0 0 0 1 1
6	Best MSE= -71.4	1 1 1 1 1 0 1 0 0 0
	Mid Tap MSE= -66.9	0 0 1 1 1 1 1 1 0 0
	Worst MSE= -42.1	1 1 0 1 0 0 0 1 1 1
7	Best MSE= -71.4	1 1 1 1 1 1 1 0 0 0
	Mid Tap MSE= -71.3	0 1 1 1 1 1 1 1 0 0
	Worst MSE= -43.3	1 1 0 1 0 1 0 1 1 1
8	Best MSE= -71.4	1 1 1 1 1 1 1 1 0 0
	Mid Tap MSE= -71.3	0 1 1 1 1 1 1 1 1 0
	Worst MSE= -51.2	1 1 0 1 0 1 1 1 1 1
9	Best MSE= -71.4	1 1 1 1 1 1 1 1 0 1
	Mid Tap MSE= -71.4	1 1 1 1 1 1 1 1 1 0
	Worst MSE= -63.8	1 1 0 1 1 1 1 1 1 1
10	Best MSE= -71.5	1 1 1 1 1 1 1 1 1 1
	Mid Tap MSE= -71.5	1 1 1 1 1 1 1 1 1 1
	Worst MSE= -71.5	1 1 1 1 1 1 1 1 1 1

Table 1 Minimum MSE Limits and Optimum Tap Placements (I)

(*) The notation indicates the placement of additional taps betweent the T spaced ones. A '1' indicates the presence of an additional tap.

Channel (II) Number of Additional Taps	MSE (in dB)	Tap Placements (*) (Hybrid T/2 taps)
1	Best MSE= -64.4	0 0 0 0 1 0 0 0 0 0
	Mid Tap MSE= -64.4	0 0 0 0 1 0 0 0 0 0
	Worst MSE= -50.5	0 0 0 0 0 0 0 0 0 1
2	Best MSE= -75.9	0 0 1 1 0 0 0 0 0 0
	Mid Tap MSE= -70.1	0 0 0 0 1 1 0 0 0 0
	Worst MSE= -59.3	1 0 0 0 0 0 0 0 0 1
3	Best MSE= -80.8	0 1 1 0 0 0 1 0 0 0
	Mid Tap MSE= -76.3	0 0 0 1 1 1 0 0 0 0
	Worst MSE= -64.9	1 1 0 0 0 0 0 0 0 1
4	Best MSE= -82.0	0 1 1 1 0 0 1 0 0 0
	Mid Tap MSE= -80.8	0 0 0 1 1 1 1 0 0 0
	Worst MSE= -67.4	1 1 0 1 0 0 0 0 0 1
5	Best MSE= -82.7	0 1 1 1 1 0 1 0 0 0
	Mid Tap MSE= -81.5	0 0 1 1 1 1 1 0 0 0
	Worst MSE= -70.2	1 1 0 1 0 0 0 0 1 1
6	Best MSE= -83.4	1 1 1 1 1 0 1 0 0 0
	Mid Tap MSE= -82.7	0 0 1 1 1 1 1 1 0 0
	Worst MSE= -73.4	1 1 0 1 0 0 0 1 1 1
7	Best MSE= -83.9	1 1 1 1 1 1 1 0 0 0
	Mid Tap MSE= -83.0	0 1 1 1 1 1 1 1 0 0
	Worst MSE= -75.2	1 1 0 1 0 1 0 1 1 1
8	Best MSE= -84.2	1 1 1 1 1 1 1 1 0 0
	Mid Tap MSE= -83.6	0 1 1 1 1 1 1 1 1 0
	Worst MSE= -77.5	1 1 0 1 0 1 1 1 1 1
9	Best MSE= -84.4	1 1 1 1 1 1 1 1 0 1
	Mid Tap MSE= -84.4	1 1 1 1 1 1 1 1 1 0
	Worst MSE= -80.6	1 1 0 1 1 1 1 1 1 1
10	Best MSE= -84.4	1 1 1 1 1 1 1 1 1 1
	Mid Tap MSE= -84.4	1 1 1 1 1 1 1 1 1 1
	Worst MSE= -84.4	1 1 1 1 1 1 1 1 1 1

Table 2 Minimum MSE Limits and Optimum Tap Placements(II)

(*) The notation indicates the placement of additional taps betweent the T spaced ones. A '1' indicates the presence of an additional tap.

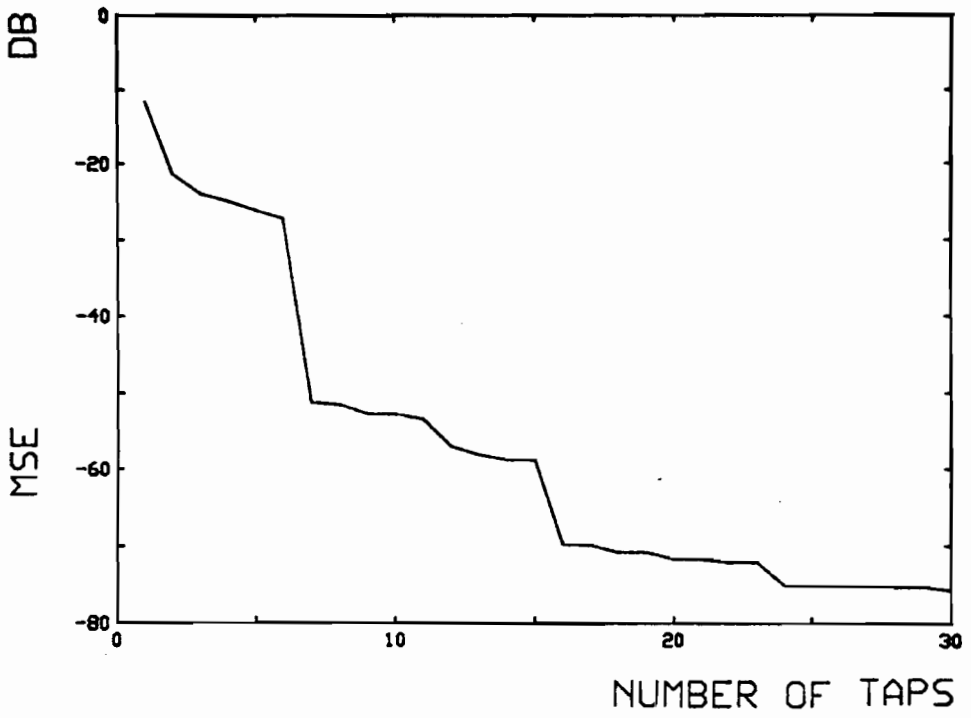

Figure 6.2 Minimum achievable MSE versus time span of the filter.

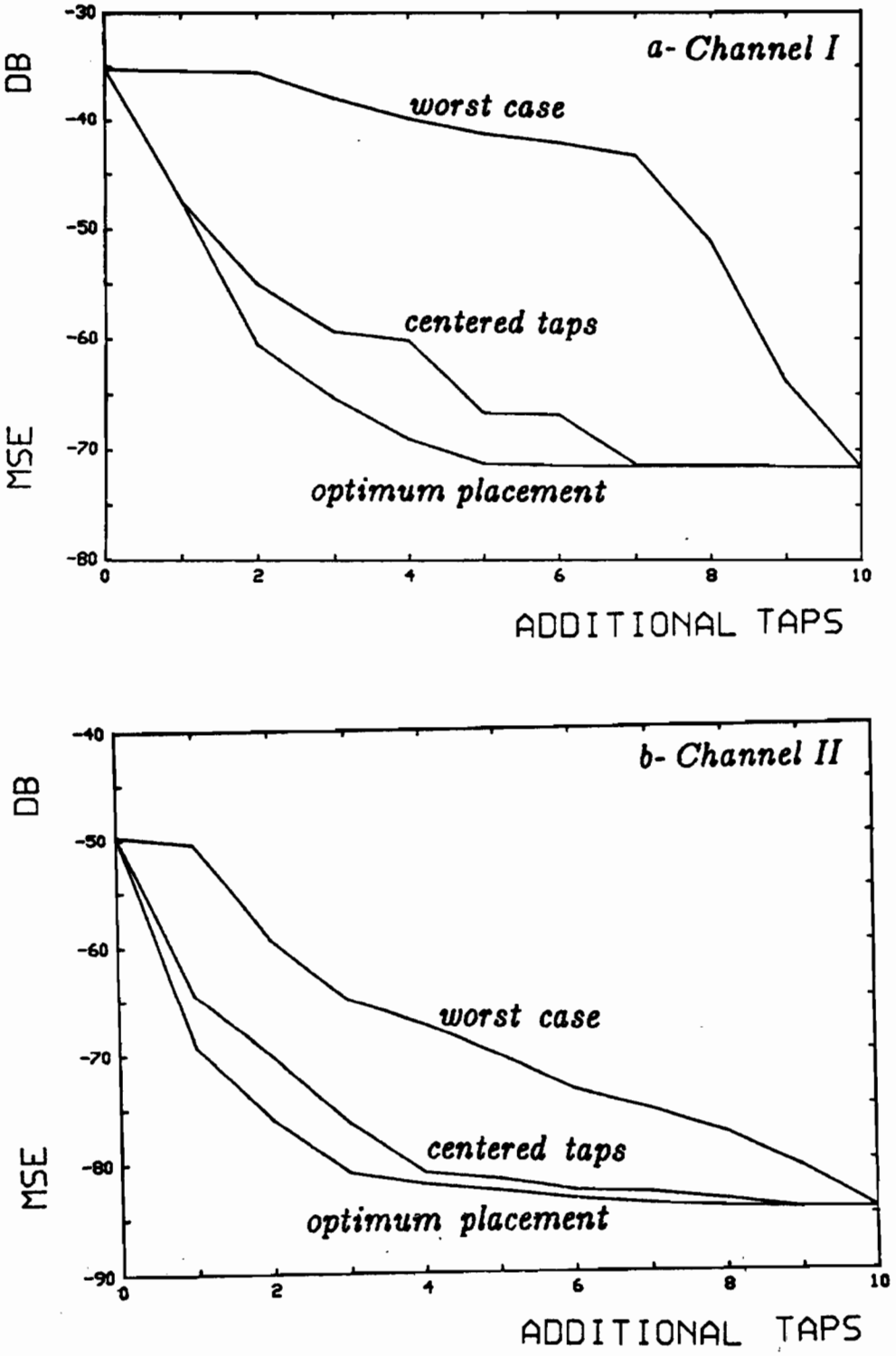

Figure 6.9 MSE limits vs Additional Tap Placement.

VI.2.1 On the Convergence of the T-Spaced, $T/2$-Spaced and HTEs

The correctness and the accuracy of the simulation methodology was checked by comparison with the theoretical expectations and with the results of similar simulation carried out by [Ungerboeck] and [Proakis]. The convergence of the adaptive transversal equalizer was studied using a signal-to-noise ratio of 30 dB which is a realistic value for the existing telephone channels [Lucky, Salz, Weldon]. A step size of 0.05 was used for a 20 tap equalizer, and the step size parameter is increased as the number of taps is reduced. Later in the chapter we will justify the inverse proportionality of the step size to the total number of taps.

In this section, the time span of the equalizer is kept at $10T$, and additional taps are inserted in the conventional T-spaced transversal equalizer. As can be seen the hybrid and the full $T/2$ equalizer have a tendency to reduce the MSE even after 2000 iterations. An important factor to be noticed is that after the first 20 iterations the equalizer is ready for decision feedback equalization, as the error rate reduces drastically at this point. In the T-spaced case, the optimum MSE is reached in about 400 iterations for both channels. The fractional $T/2$ case has a much smaller minimum achievable MSE. In order to see the hybrid effect, only one tap was inserted in the T-spaced equalizer (Figure 6.4). But when three or four taps are inserted (the placement of which are explained above) the hybrid equalizer performs essentially as well as the $T/2$ equalizer, except with a slight offset MSE (see Figure 6.5). The results indicate that the convergence rate of the hybrid equalizer is similar to that of the $T/2$-spaced equalizer, particularly with respect to the initial decrease of the mean-square error. The performance of the hybrid equalizer falls in between the conventional and $T/2$ equalizer. For the channels simulated in our experiments it is seen that three-additional-tap hybrid equalizer performs nearly as well as the $T/2$ case, which has seven more taps than the latter.

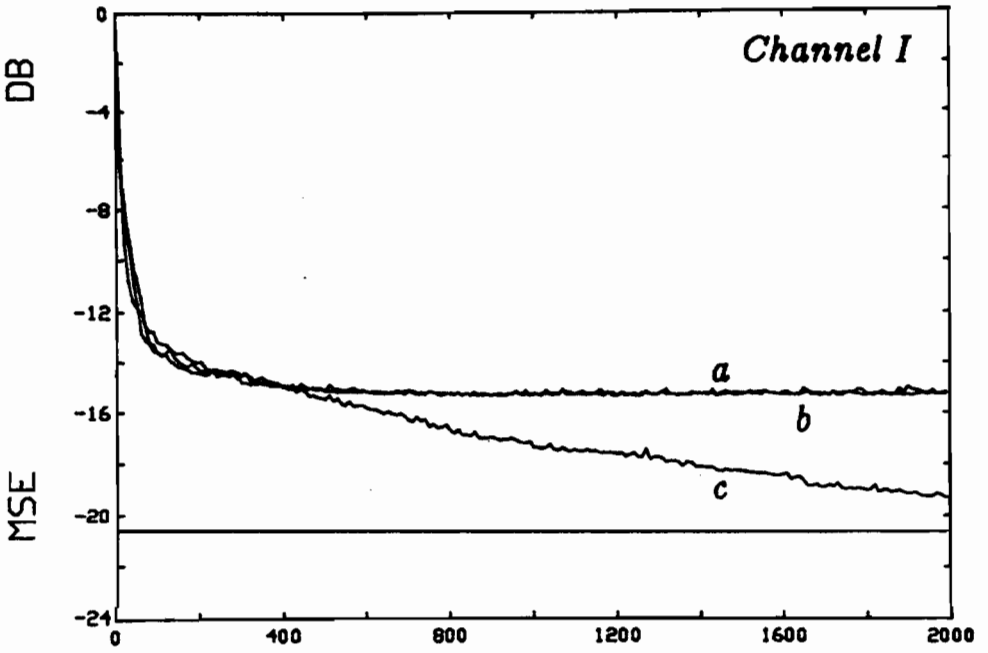

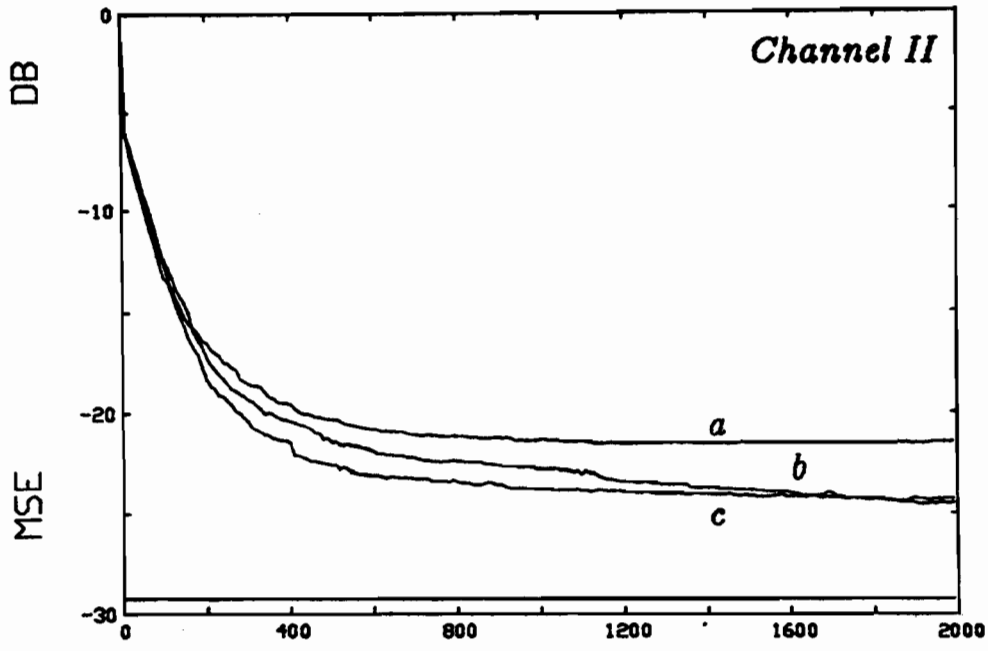

Figure 6.4 Comparison with one additional tap.
a- T-spaced,
b- worst placement of the additional tap,
c- best placement of the additional tap.

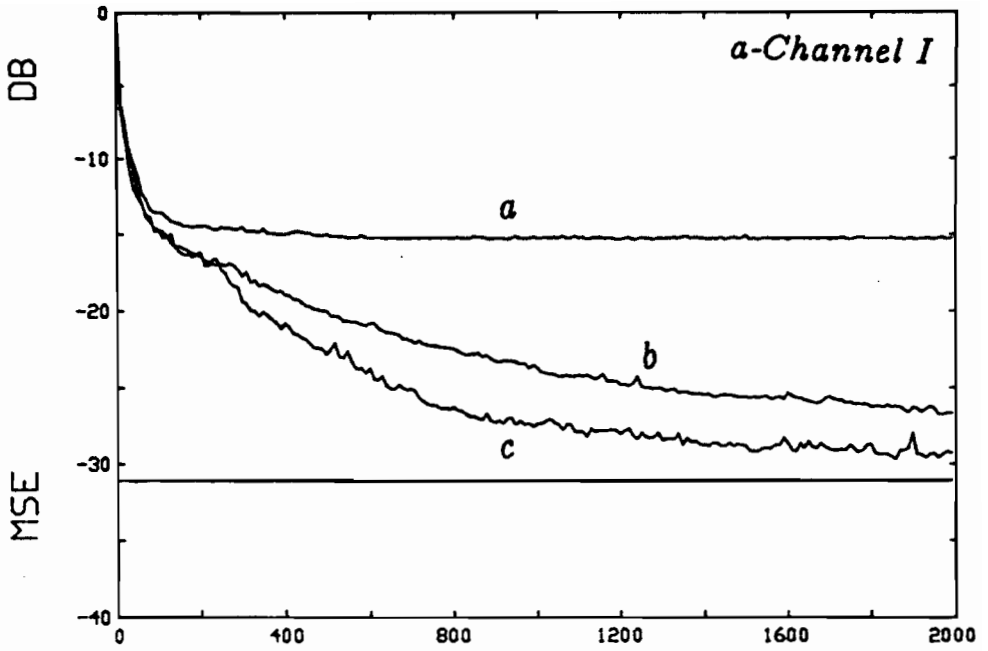

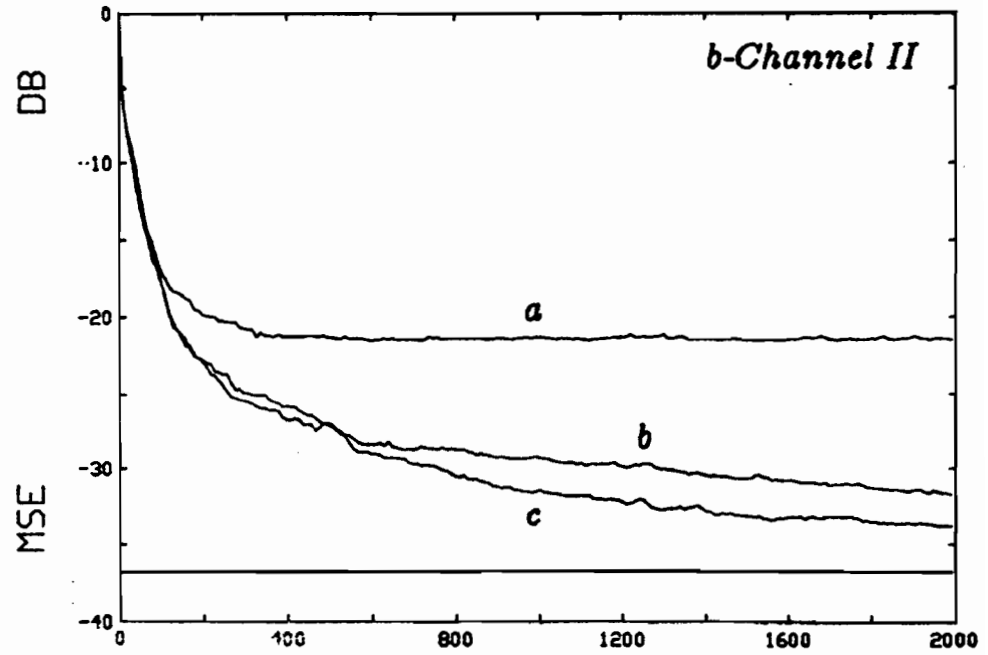

Figure 6.5 Comparison of the three cases.
a- T Spaced Equalizer
b- Hybrid Equalizer with three additional taps
c- T/2 Spaced Equalizer

VI.3 The Excess-MSE(e_Δ^2) and the Stability Limits

VI.3.1 Minimum MSE versus Number of taps

In this section, we show that, as the number of taps are increased, the noise due to fluctuation of the additional taps increases the MSE. One of the reasons for this phenomenon is the tap coefficient updating algorithm. The tap fluctuations about their optimal values in the tap updating procedure are due to the use of noisy estimates rather than the true gradient components. This leads to an increase in the mean-square error at the output of the receiver. As the optimum MSE is approached, the amplitude of the fluctuations increases. The above mentioned effect is shown in Figure 6.6(a,b,c) where 20, 40 and 50 tap equalizers were simulated, and 5000 training iterations were carried out to determine the steady state excess MSE for a constant step size. The fluctuations are most noticable in steady-state when these plots are studied. From the simulations it is apparent that the excess MSE is nearly proportional to the total number of taps.

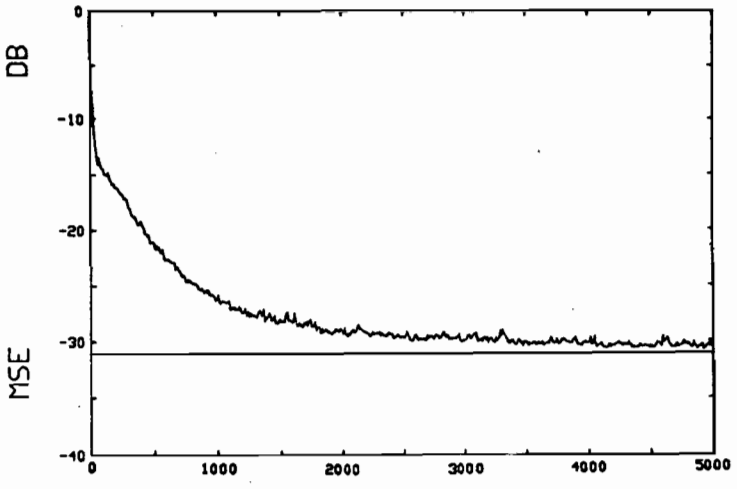

a- 20 Taps

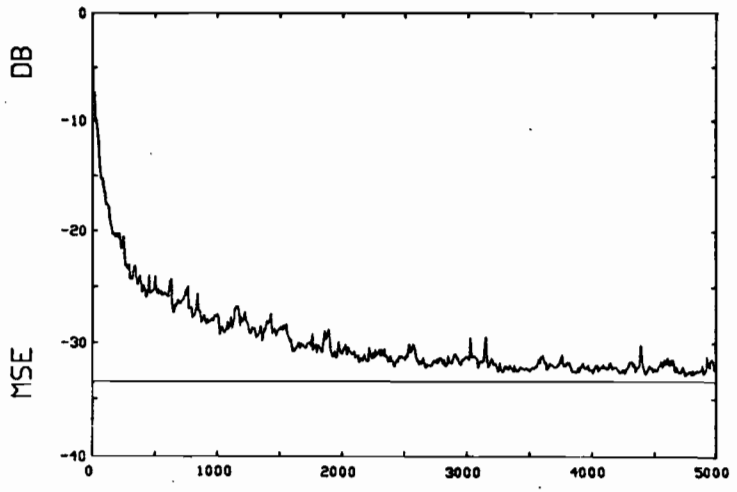

b- 40 Taps

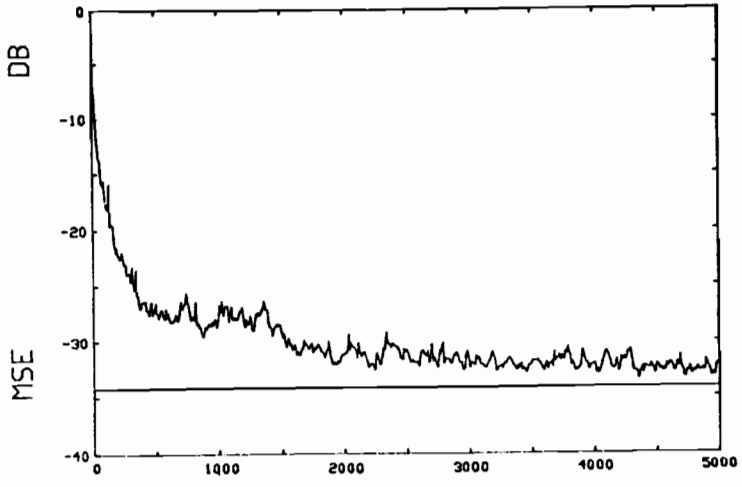

c- 50 Taps

Figure 6.6 Performance of the T/2 equalizer with different number of taps.

VI.3.2 Effects of Step Size on Excess-MSE and Stability

The step size is a major concern for the optimization of the system. Although, a fast convergence is realized with a larger step size, the fluctuations (excess MSE) are considerably more at the later portion of the operation. If the step size is large (the absolute size is determined by the number of taps and the channel noise level) it has been observed that the equalizer is unstable, and that it diverges from the optimal values after a few iterations (Figure 6.7). This represents a serious breakdown for a decision-directed operation where the equalizer is in the receiving stage. In the following figures only the step size of the equalizer has been changed. In the first part of Figure 6.7 a step size of 0.05 has been used and resulted in a smooth convergence and a steady minimum MSE. In the other two cases step sizes of 0.10 and 0.15 were used. Although this results in a faster rolloff in the beginning, larger step size gives rise to a higher steady-state mean-square error as well as the fluctuations about the optimal tap values have large peaks compared to the step size of 0.05 case.

The same simulation is also carried out when the number of taps were changed from 20 to 30 to 40 in order to see the constraint on the step size for stability. As seen in Figures 6.8 and 6.9, it can be observed that for different number of taps the equalizers show the following results; (i) For a larger number of taps the step size has to be smaller for a smooth performance, (ii) The equalizers with fewer number of taps can use a much larger step size giving a more rapid adaptation. The maximum step size is determined by the total number of taps which is determined by the stability limit.

The simulations carried out in this chapter have been done using the two channels. The results for channel II have not been included as they show similar trends. In the next chapter, we present a general summary of the thesis as well as the conclusion derived from the theory, expectations and results.

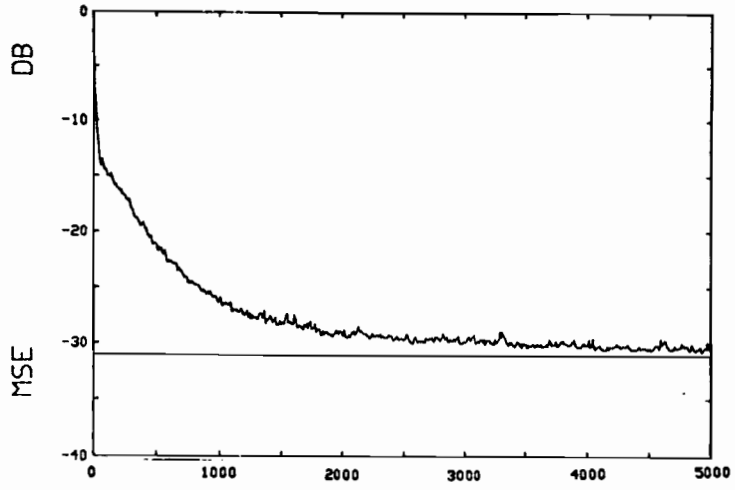

a- Step size = 0.05

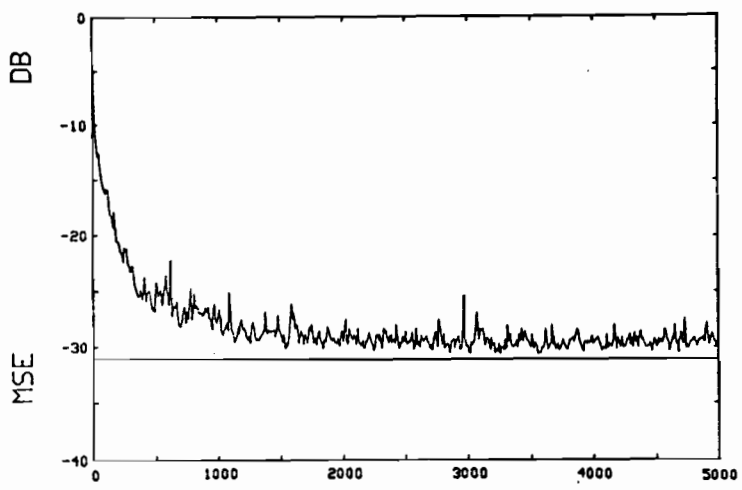

b- Step size = 0.10

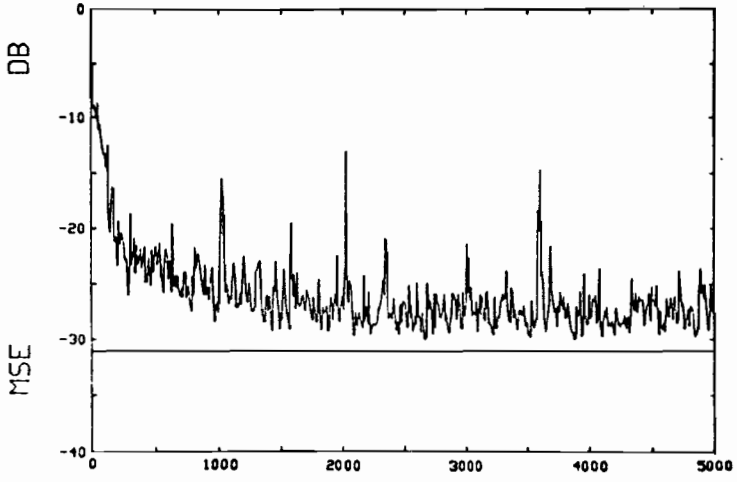

c- Step size = 0.15

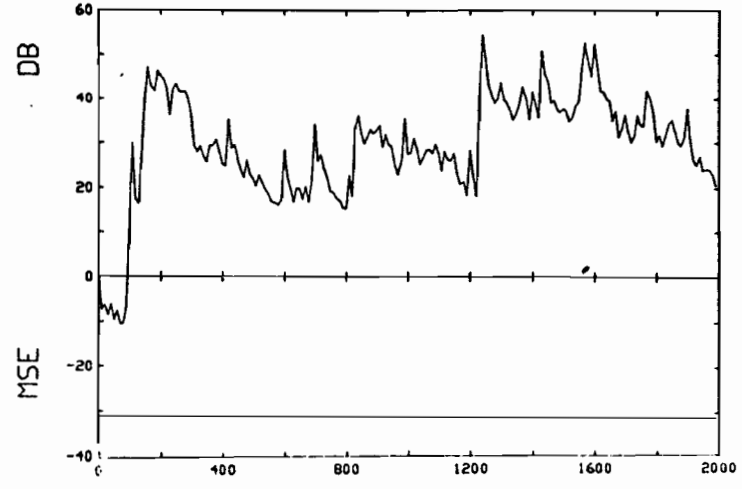

d- Step size = 0.19

Figure 6.7 Performance of the 20 tap T/2 equalizer with different step sizes (Channel I).

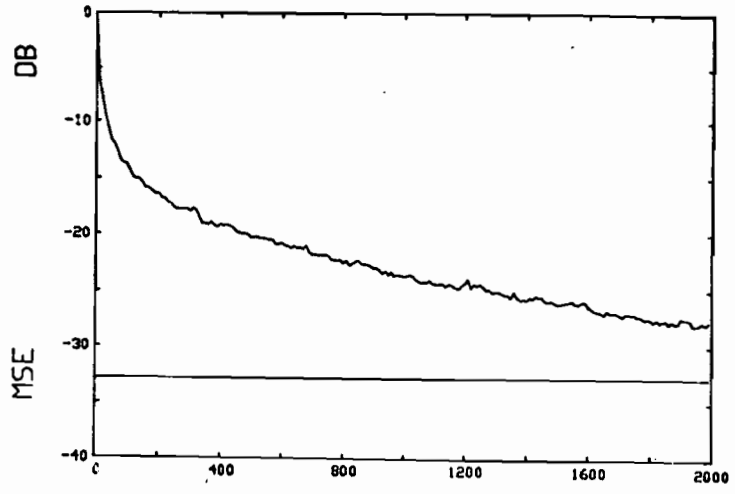

a- Step size = 0.03

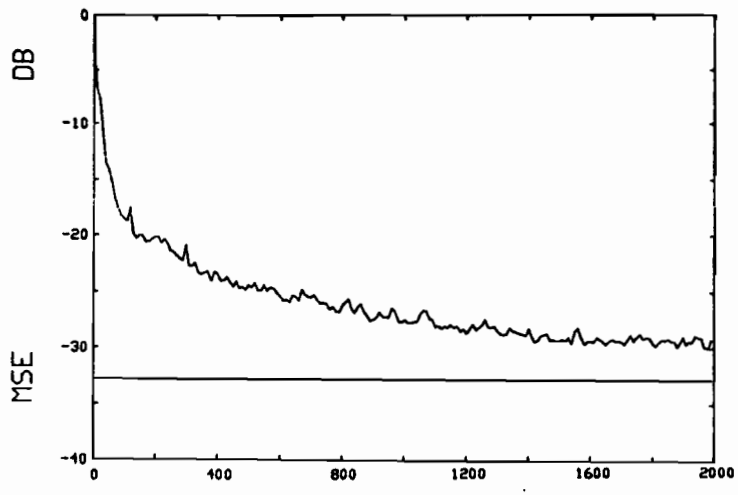

b- Step size = 0.05

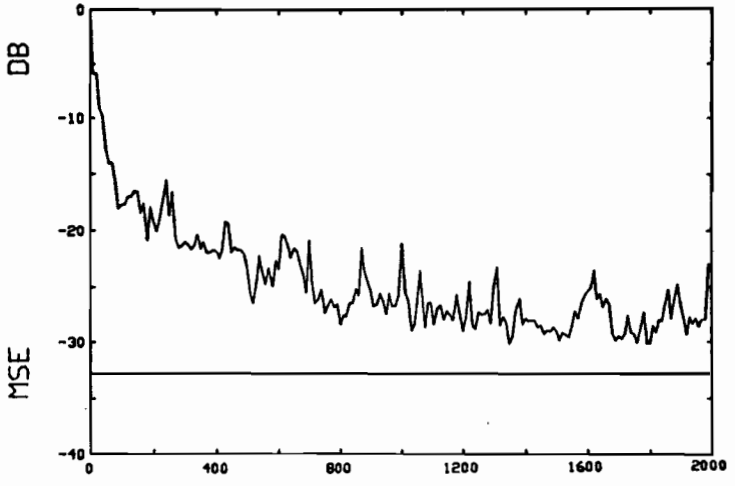

c- Step size = 0.10

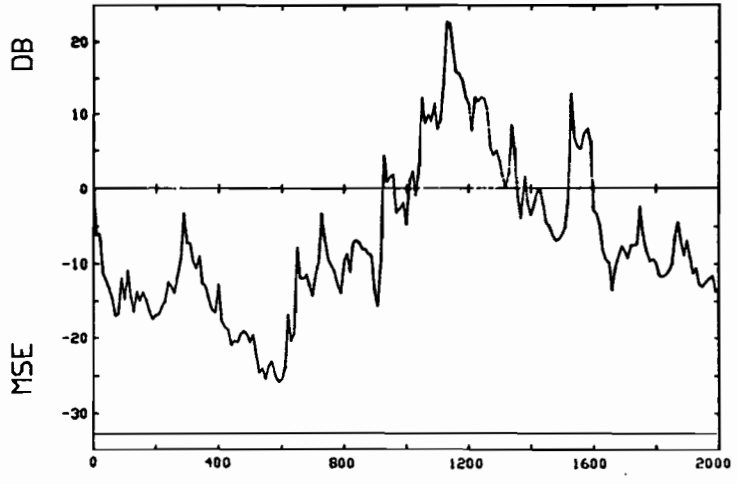

d- Step size = 0.13

Figure 6.8 Performance of the 30 tap T/2 equalizer with different step sizes (Channel I).

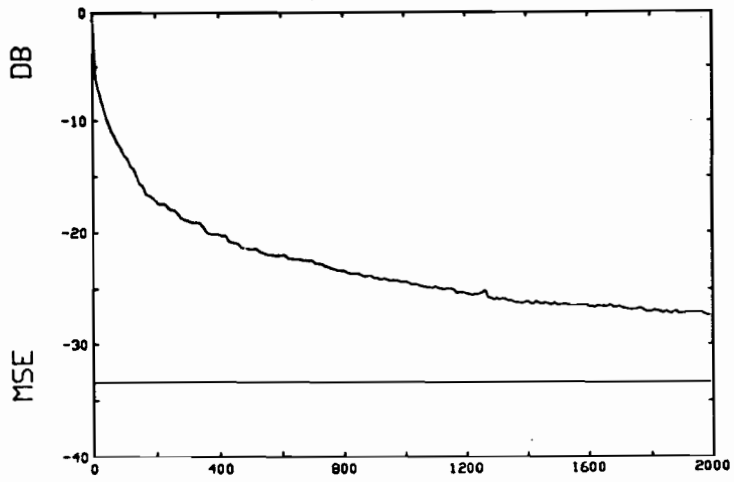

a- Step size = 0.02

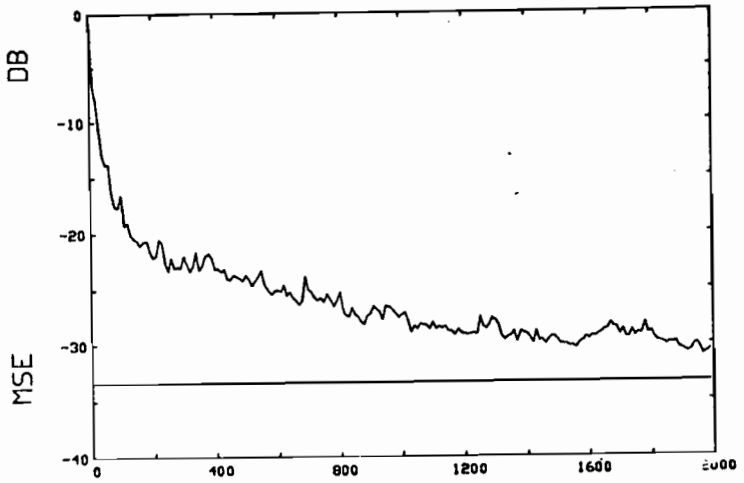

b- Step size = 0.05

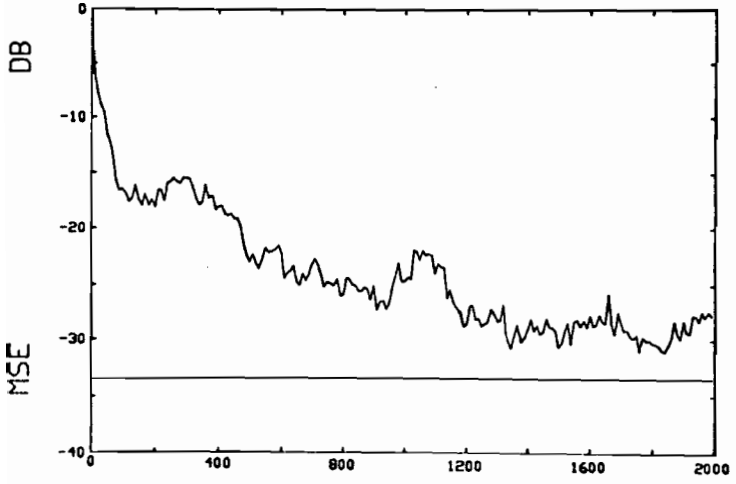

c- Step size = 0.08

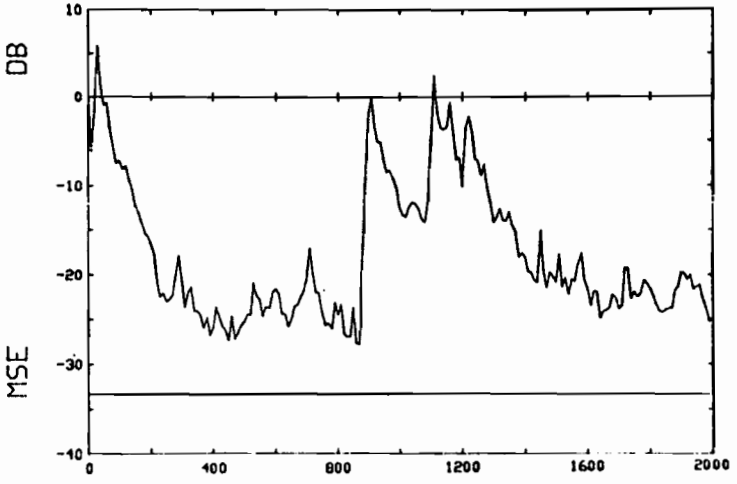

d- Step size = 0.09

Figure 6.9 Performance of the 40 tap T/2 equalizer with different step sizes (Channel I).

SUMMARY and CONCLUSION

In this thesis we introduced a generalized digital transmission system and then studied the optimization of such a system. A receiver optimization strategy is chosen because the channel characteristics and the behaviour of noise is in general unknown. Thus we started analysing the receiver and came up with a suboptimal realizable receiver. This involves a low-pass filter, a transversal filter and a decision unit. Once the form of the system is known, the low-pass filter and the decision unit are placed in the receiver. We have concentrated on the transversal filter section of the receiver. The weighted sums of the past and future samples (relative to the reference tap) of the signal are available at the output of the transversal filter. The elimination of intersymbol interference can be handled once the tap weights of the transversal filter are derived. Inorder to find these tap coefficients we have selected to minimize the mean-square error. This led to a derivation of a generalized equalizer model which has arbitrary tap positions. This analysis was used when the particular equalizers were studied, the T-spaced, $T/2$-spaced and the hybrid cases. We have tried to extract the properties of the above mentioned equalizers considering their frequency responses, the autocovariance matrix and their eigenvalues, and the mean-square error. For each case the equalizer is assumed to be infinite.

The algorithms that can be applied to find the tap coefficients iteratively were introduced. The steepest descent method was discussed and used in the simulations. The convergence, the stability constraints were also discussed. The dependence of

the number of taps as well as the step size to the convergence behaviour of the equalizer was shown. One of the variables namely the excess mean-square error was derived to prove some results.

The simulation results showed the benefits and the limitations of the three equalizers studied. It has been observed that the step size is an important factor in stability and the convergence of the equalizers. When a small step size is used, the convergence to the optimum tap settings is reached very slowly, and the fluctuations around the minimum mean-square error is small. A larger step size gives rise to a faster adaptation yet it has a considerable excess mean-square error at the steady state. It is also apparent from the simulations that the number of taps has an important role in the performance of the adaptation behaviour of the equalizers. The step size and the number of taps are directly related in the performance. When the number of taps is large, the excess mean-square error increases, and for particular conbination of step size and number of taps, it is shown that the equalizer is unstable. Which in turn shows the inverse proportionality between the step size and the number of taps. The superiority of the hybrid type equalizer comes into effect at this moment. Since the convergence rate depends on the step size, one can obtain larger step sizes than $T/2$ case since in has less number of taps for the same timespan.

Therefore the final word we will state is that the hybrid equalizer has most of the properties of the $T/2$ spaced equalizer in terms of convergence, and superior in terms of stablity. Also having less number of taps reduces the excess mean-square error as well as the complexity of the system. Although we have not studied the effects of the sampling phase when a hybrid equalizer is used, the study by Nattiv shows that it is much less dependent compared to the conventional equalizer.

LITERATURE

[1] G. Ungerboeck, "Fractional Tap-Spacing Equalizers and Consequences for Clock Recovery in Data Modems", IEEE Trans. on Comm. ,vol. Com-24, pp. 856-864, August 1976.

[2] G. Ungerboeck, "Theory on the Speed of Convergence in Adaptive Equalizers for Digital Communication", IBM J. Res. Develop. , vol. V-16, pp. 546-555, November 1972.

[3] J. G. Proakis, "An Adaptive Receiver for Digital Signalling Through Channels With Intersymbol Interference", IEEE Trans. on Information Theory, vol. IT-15, pp. 484-497, July 1969.

[4] S. U. H. Qureshi and D. Forney, "Performance and Properties of T/2 Equalizer", NTC '77, pp. 11:1.1-11:1.9, 1977.

[5] R. D. Gitlin and S. B. Weinstein, "Fractional Spaced Equalization: An Improved Digital Transversal Equalizer", BSTJ,vol. 60, pp. 275-294, February 1981.

[6] M. S. Mueller, "Least-Squares Algorithms for Adaptive Equalizers", BSTJ,vol. 60, pp. 193-213, October 1981.

[7] B. Widrow, *Adaptive Filters*, in " Aspects of Network and System Theory", Kalman R. E. and Declaris N.(Eds.), Holt Rinehart and Winston, pp. 563-587, 1971.

[8] H. Rudin, "Automatic Equalization Using Transversal Filters", IEEE Spectrum, pp. 53-59, January 1967.

[9] O. S. Kosovych and R. L. Pickholtz, "Automatic Equalization Using

a Successive Overrelaxation Iterative Technique", IEEE Trans. on Information Theory,vol. IT-21, pp. 51-58, January 1975.

[10] R. W. Lucky, J. Salz and E. J. Weldon, " Principals of Data Communication", New York, McGraw-Hill, 1968.

[11] R. W. Lucky, "Automatic Equalization for Digital Communication.", BSTJ, vol. 44, p. 547, 1965.

[12] R. W. Lucky, "Techniques for Adaptive Equalization of Digital Communication Systems.", BSTJ, vol. 45, p. 255, 1965.

[13] R. W. Lucky and H. R. Rudin, "An Automatic Equalizer for General-Purpose Communication Channels.", BSTJ, vol. 46, p. 2197, 1967.

[14] A. Gersho, "Adaptive Equalization for Highly Dispersive Channels for Data Transmission", BSTJ, vol. 48, p. 55, 1969.

[15] D. Hirsch and W. J. Wolf, "A Simple Adaptive Equalizer for Efficient Data Transmission.", IEEE Trans. on Communication, vol. Com-18,5 1970.

[16] R. W. Chang, "A New Equalizer Structure for Fast Start-up Digital Communication.", BSTJ, vol. 50, p. 143, 1971.

[17] T. J. Schonfeld and M. Schwartz, "A Rapidly Converging First-Order Training Algorithm for an Adaptive Equalizer", IEEE Trans. on Information Theory, vol. IT-21, pp. 431-439, July 1971.

[18] J. E. Mazo, "On the Independence Theory of the Equalizer Convergence", BSTJ, vol. 58, pp. 963-983, May-June 1979.

[19] T. Ericson, "Structure of Optimum Receiving Filters in Data

Transmission Systems", IEEE Tran. on Information Theory, vol. IT-17, pp. 352-353, May 1971.

[20] M. S. Mueller, "On the Rapid Initial Convergence of Least-Squares Adjustment Algorithms", BSTJ, vol. 60, pp. 2345-2359, December 1981.

[21] T. J. Schonfeld and M. Schwartz, " Rapidly Converging Second-Order Tracking Algorithms for Adaptive Equalization", IEEE Trans. on Information Theory, vol. IT-17, pp. 572-579, September 1971.

[22] M. Nattiv, "Fractional Tap-Spacing Equalizers for Data Transmission", M. Eng. Thesis, McGill University, Electrical Engineering Dept. , 1980.

APPENDIX

A.1 The Derivation of Equation (3.16)

We start from the mean of the square error, as in equation (3.15)

$$\overline{|e_k|^2} = \overline{(y_k - d_k)\ (y_k{}^* - d_k{}^*)}. \tag{A.1.1}$$

Making use of the vector notations defined in the related sections, one obtains (*)

$$\overline{|e_k|^2} = \overline{(\bar{C}^H \bar{x}^* - d_k{}^*)\ (\bar{x}^T \bar{C}^T - d)}. \tag{A.1.2}$$

By defining the following matrix and vector

$$A \triangleq \overline{\bar{x}_k{}^*\ \bar{x}_k^T},$$

$$\bar{\alpha} \triangleq \overline{\bar{x}_k\ d_k{}^*},$$

the result of the above mean-square error term is of the following form

$$\overline{|e_k|}^2 = \bar{C}^H A\ \bar{C} - \bar{\alpha}^T \bar{C} - \bar{C}^H \bar{\alpha}^* + \overline{|d_k^2|}, \tag{A.1.3}$$

All of the vectors in the above equation are complex, i.e. $\bar{C} = Re\{\bar{C}\} + jIm\{\bar{C}\}$. To minimize the mean-square error $\overline{|e|}^2$ term with respect to $\bar{C}$, we have to differentiate it with respect to $Re[c_k]$ and $jIm[c_k]$ for every k. We define complex functions that,

---

* $[.]^H$ is the conjugate-transpose operation.

$$\frac{\partial\overline{|e_k|^2}}{\partial Re\{\bar{C}\}} + j\frac{\partial\overline{|e_k|^2}}{\partial Im\{\bar{C}\}} = A\bar{C}^T - \bar{C}^*A^T - \bar{\alpha}^T - \bar{\alpha}^* + j(\bar{\alpha}^* - \bar{\alpha} + \bar{C}^TA - \bar{C}^*A) \qquad (A.1.4)$$

$$= 2Re(A\bar{C}) - 2Re(\bar{\alpha}) + j(-2Im(\bar{\alpha}) + 2Im(\bar{C}A))$$

$$= 2A\bar{C} - 2\bar{\alpha}. \qquad (A.1.5)$$

Setting the derivative to zero,

$$2A\bar{C}_{opt} - 2\bar{\alpha} = 0$$

Then, $\bar{C}_{opt} = A^{-1}\bar{\alpha}$ **and the minimum mean-square error can be written as**

$$\overline{|e_k|^2}_{min} = \overline{|d|^2} - \bar{\alpha}^H\bar{C}_{opt} \qquad (A.1.6)$$

A.2 The derivation of Equation(3.20)

The input signal to the receiver is

$$x(t) = \sum_n a_n h(t - nT) + n(t). \tag{A.2.1}$$

Inserting the above equation in (3.17) we get

$$\begin{aligned} A_{k,l} = \sum_i \sum_j \overline{a_i^* a_j}\ & h^*[(k - D_k - i + \frac{\tau}{T})T]\ h^*[(k - D_l - j + \frac{\tau}{T})T] \\ & + n^*[(k - D_k + \frac{\tau}{T})T]\ n[(k - D_l + \frac{\tau}{T})T]. \end{aligned} \tag{A.2.2}$$

Using the definitions

$$\Phi_{aa}(i - j) \triangleq \overline{a^*_i\ a_j},$$

$$\Phi_{nn}[(D_k - D_l)T] \triangleq n^*[(k - D_k - \frac{\tau}{T})T]n[(k - D_l - \frac{\tau}{T})T].$$

and letting $m = i - j$ and $n = k - j$, we get the following

$$\begin{aligned} A_{k,l} = \sum_m \Phi aa(m) \sum_n & h^*[(n - m - D_k + \frac{\tau}{T})T] \\ & h[(n - D_k + \frac{\tau}{T})T] + \Phi_{nn}[(D_k - D_l)T]. \end{aligned} \tag{A.2 3}$$

The derivation of equation (3.20) is shown above. Equation (3.21) can also be derived using the same steps starting from Eq. (3.18).

A.3 The derivation of Equation (3.25)

Starting with the transform definition

$$h(t) = \int_{-\infty}^{+\infty} H(f)\ \exp(j2\pi ft)\ df, \tag{A.3.1}$$

we substitute it in equation (A.II-3). By using this substitution and by carrying out the integrations first and then summing over m and n, we come up with

$$A = \int_{-\infty}^{+\infty}\int_{-\infty}^{+\infty} H(f)H(\lambda)\sum_m \Phi_{aa}(m)\exp(j2\pi fmT)$$
$$\sum_n \exp(j2\pi n(\lambda - f)T)\exp(-j2\pi(f-\lambda)\tau)\exp(j2\pi fD_kT)\exp(-j2\pi\lambda D_lT)]\ d\lambda\ df + \sigma_n^2\delta_{k,l} \tag{A.3.2}$$

Define the data source power spectrum as

$$\Phi_{aa}(f) \triangleq \sum_m \Phi_{aa}(m)\exp(j2\pi fmT), \tag{A.3.3}$$

also

$$\sum_n \exp(-j2\pi(f-\lambda)Tn) = \frac{1}{T}\sum_i \delta(\lambda - f - \frac{i}{T}). \tag{A.3.4}$$

Using the above equations, if the integration is carried out on successive intervals of length $1/T$, we come up with

$$A_{k,l} = \frac{1}{T}\int_{-\frac{1}{T}}^{\frac{1}{T}} H_{eq}^k(f)^*\ H_{eq}^l(f)\ \Phi_{aa}(f)\ df, \tag{A.3.5}$$

which is equation (3.25), where

$$H_{eq}^k \triangleq \sum_i H(f+\frac{i}{T})\exp(-j2\pi(f+\frac{i}{T})D_lT)\exp(j2\pi\frac{\tau}{T}), \tag{A.3.6}$$

is the Nyquist equivalent for $H(f)\exp(j2\pi ft)$.

A.4 Proof of Theorem 1

Proof:

Assume that λ_A is an eigenvalue of A matrix, and that u is its corresponding eigenvector. By definition

$$A \triangleq \overline{\bar{x}_k^* \bar{x}_k^T}. \tag{A.4.1}$$

Note that

$$\bar{u}^H A\ \bar{u} = \lambda_A\ \bar{u}^H \bar{u}. \tag{A.4.2}$$

Inserting the definition for A, we have

$$\overline{\bar{u}^H \bar{x}_k^*\ \bar{x}_k^T \bar{u}} = \lambda_A\ \bar{u}^H \bar{u}, \tag{A.4.3}$$

which can be put in the following form,

$$\overline{|\bar{x}_k^T\ \bar{u}|}^2 = \lambda_A\ \bar{u}^H \bar{u}. \tag{A.4.4}$$

Now, defining

$$q_k \triangleq \bar{x}_k^T\ \bar{u}, \tag{A.4.5}$$

which gives,

$$\overline{|q_k|^2} = \lambda_A \bar{u}^H \bar{u}. \tag{A.4.6}$$

When the z-transform of q_k , $Q(f)$ is computed around the unit circle in the z-plane then

$$Q(f) = U(f)\ X_{eq}(f) \tag{A.4.7}$$

For $X_{eq}(f)$ defined as before

$$X_{eq}(f) = \sum_i X(f + i/T). \tag{A.4.8}$$

By using Parseval's theorem and Eqn. (2.9),

$$\begin{aligned} \overline{|q_k|^2} &= \sigma_a^2 \int_{-\frac{1}{2T}}^{+\frac{1}{2T}} U(f)\ H_{eq}(f)\ df \\ &= \lambda_A \int_{-\frac{1}{2T}}^{+\frac{1}{2T}} U(f)|^2 df. \end{aligned} \tag{A.4.9}$$

Since we were given that

$$m \leq |H_{eq}(f)|^2 \leq M.$$

We get

$$m \leq \lambda_A \leq M. \tag{A.4.10}$$